

QUEST#4X: an extension of QUEST#4 for benchmarking multireference wavefunction methods

Yangyang Song,[†] Ning Zhang,[†] Yibo Lei,[‡] Yang Guo,[†] and Wenjian Liu^{*,†}

[†]*Qingdao Institute for Theoretical and Computational Sciences, School of Chemistry and
Chemical Engineering, Shandong University, Qingdao 266237, China*

[‡]*Key Laboratory of Synthetic and Natural Functional Molecule of the Ministry of Education,
College of Chemistry & Materials Science, Shaanxi key Laboratory of Physico-Inorganic
Chemistry, Northwest University, Xi'an 710127, China*

E-mail: liuwj@sdu.edu.cn

Abstract

Given a number of datasets for evaluating the performance of single reference methods for the low-lying excited states of closed-shell molecules, a comprehensive dataset for assessing the performance of multireference methods for the low-lying excited states of open-shell systems is still desired. For this reason, we propose an extension (QUEST#4X) of the radical subset of QUEST#4 [J. Chem. Theory Comput. 2020, 16, 3720] to cover 110 doublet and 39 quartet excited states. Near-exact results obtained by iCIPT2 (iterative configuration interaction with selection and second-order perturbation correction) are taken as benchmark to calibrate SDSCI (static-dynamic-static configuration interaction) and SDSPT2 (static-dynamic-static second-order perturbation theory), which are minimal MRCI and CI-like perturbation theory, respectively. It is found that SDSCI is very close in accuracy to ic-MRCISD (internally contracted multireference configuration interaction with singles and doubles), although its computational cost is just that of one iteration of the latter. Unlike most variants of MRPT2, SDSPT2 treats single and multiple states in the same way, and performs similarly as MS-NEVPT2 (multi-state n-electron valence second-order perturbation theory). These findings put SDSCI and SDSPT2 on a firm basis.

1 Introduction

The last decades have witnessed fast progresses in the development of both wavefunction- and density-based quantum chemical methods for describing electronic structures of chemical systems. It is generally true that the strengths and weaknesses of each of such methods should be uncovered before they can be applied safely to unknown problems. To this end, some standardized datasets should be established, such that they can be employed to identify the error bars of a given method. A dataset is composed of two ingredients, target systems and reference data. The former refers to chosen molecules and their properties, whereas the latter refers to corresponding experimental or highly accurate theoretical values. The target systems can be classified according to the simple criteria, (1) closed-shell (CS) or open-shell (OS), (2) main group (MG) or transition metal (TM), (3) ground state (GS) or excited state (ES), thereby leading to 8 types of datasets (see Fig. 1), to which the available datasets can be assigned. It can be seen from Table 1 that there exist at least 123 datasets for ground states of CS-MG¹⁻¹⁰¹, OS-MG^{1-24,102}, and CS/OS-TM^{1-8,103-123} (including lanthanides^{109,117,118} and actinides^{110,116}). Such datasets were mainly used to calibrate SR methods^{1-21,25-118,123-139}, especially density functional theory (DFT)^{1-18,25-82,103-113}, although some of them were also used to assess the performance of MR methods.^{22,23,100,101,115,117,118,140-142} In parallel, there exist 73 datasets oriented to excited states of CS-MG^{4-8,143-197}, OS-MG^{4-8,143-147,198-202}, CS-TM^{4-8,143,203-207}, and OS-TM^{4-8,143,203,204,208-210}, aiming to calibrate both SR^{4-8,143-146,148-196,198-209,211-215,215-239} and MR^{146,147,185-197,203-207,209,210,238,240-252} methods.

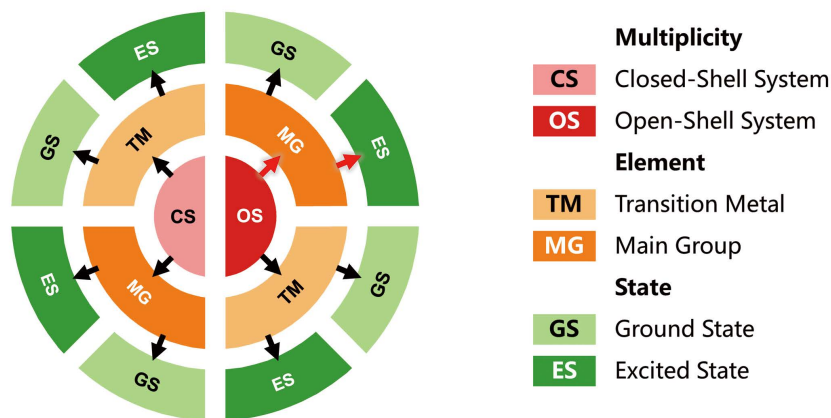


Figure 1: Classification of datasets

Table 1: Up-to-date datasets*

Ground State	
CS-MG	Refs. 1–101
OS-MG	Refs. 1–24,102
CS-TM	Refs. 1–8,103–122
OS-TM	Refs. 1–8,103–118,123
Excited State	
CS-MG	Refs. 4–8,143–197
OS-MG	Refs. 4–8,143–147,198–202
CS-TM	Refs. 4–8,143,203–207
OS-TM	Refs. 4–8,143,203,204,208–210

* CS: closed-shell; OS: open-shell; MG: main group; TM: transition metal.

As for the reference data, the very first point to be realized lies in that experimental measurements often cannot be taken as they stand. For instance, experimentally measured 0-0 transition energies cannot directly be compared to theoretically calculated vertical excitation energies (VEE), which are not observable. Instead, geometric and vibrational effects must be added to theoretical VEEs or subtracted from experimental 0-0 transition energies.^{143,153,156,166,171,176,179,253,254} The lack of sufficient experimental data necessitates the use of some high-level methods as the reference for low-level meth-

ods. However, this is not always reliable. It is often the case that the chosen high-level method is itself not sufficiently accurate. For instance, the near-exact iCIPT2/TZVP (iterative configuration interaction with selection and second-order perturbation^{255,256}) calculations¹⁴⁷ of the singlet VEEs of the dataset¹⁹⁶ overturned the recommendation of using the CASPT2/TZVP rather than the CC3/TZVP values as the theoretical best estimates (TBE),¹⁹⁶ which was based simply on the extent of MR characters.

Close inspections of the up-to-date datasets (see Table 1) reveal that there exists only one dataset¹⁴⁷ for calibrating MR methods for the excited states of open-shell organic systems. As such, more comprehensive datasets are highly desired. As a first try towards this goal, we start with the QUEST#4 dataset,¹⁴⁵ which contains 24 organic radicals (see Fig. S1 in the Supporting Information). Since only 51 doublet excited states were reported therein, an immediate extension is to cover more excited states, both doublet and quartet. Such an extended dataset, covering 110 doublet and 39 quartet states for the 24 radicals, is to be dubbed QUEST#4X. The VEEs calculated by iCIPT2 will be employed to calibrate MR methods [SS/MS-NEVPT2 (single/multi-state second-order n-electron valence state perturbation theory),^{257,258} SDSPT2 (static-dynamic-static (SDS) second-order perturbation theory),^{259,260} SDSCI,²⁵⁹ and ic-MRCISD (internally contracted multireference configuration interaction with singles and doubles)²⁶¹], as well as the spin-adapted open-shell TD-DFT.²⁶²⁻²⁶⁴ The SDSCI, SDSPT2, and iCIPT2 methods are first recapitulated in Sec. 2, which is followed by computational details in Sec. 3. The results are analyzed in Sec. 4. The paper is closed with concluding remarks in Sec. 5.

2 Computational Methods

The (restricted) static-dynamic-static (SDS) family of methods for strongly correlated systems of electrons has been presented at length before.^{147,265} Therefore, it is only necessary to explain here their internal relations. In the first place, no matter how many electrons

and how many orbitals are to be correlated, SDSCI²⁵⁹ always constructs and diagonalizes a $3N_p$ -by- $3N_p$ matrix for N_p states simultaneously. Therefore, SDSCI is a minimal MRCI resulting from the combination of the good of perturbation theory, intermediate Hamiltonian, and configuration interaction. Taking the N_p eigenvectors of SDSCI as new references and repeating SDSCI until convergence, we obtain iCI,²⁶⁶ where each iteration accesses a space that is higher by two ranks than that of the preceding iteration. That is, up to $2M$ -tuple excitations (relative to the initial reference space) can be accessed if M iterations are carried out. Because of the variational nature, any minor loss of accuracy stemming from the contractions can be removed by carrying out some micro-iterations. In other words, by controlling the numbers of macro- and micro-iterations, iCI will generate a series of contracted/uncontracted single/multireference CISD $\cdots 2M$, with the resulting energy being physically meaningful at each level. It has been shown both theoretically and numerically that iCI can converge monotonically and quickly from above to FCI, even when starting with a very poor initial guess. As such, iCI can be interpreted as an exact solver of FCI. Further combined with the selection of configurations for static correlation and perturbation correction for dynamic correlation, we obtain the near-exact iCIPT2.^{255,256} On the other hand, if the QHQ block of the SDSCI matrix (i.e., matrix elements within the first-order interacting space) is replaced by QH_0Q , we obtain SDSPT2,^{259,260} a CI-like MRPT2 that treats single and multiple states in the same way and is particularly advantageous when a number of states are nearly degenerate (because of the sufficient relaxation of the reference coefficients).²⁶⁰ In short, if the SDSCI calculation is to be performed, we would obtain SDSPT2 results for free. The latter further yields, e.g., MS-NEVPT2 results for free, because all matrix elements required by MS-NEVPT2²⁵⁸ are already available. Moreover, SDSCI can be taken as a start of ic-MRCISD, so as to facilitate the convergence of the latter. As a matter of fact, the increments of the ic-MRCISD iterations clearly indicate the accuracy of SDSCI. Given so many good features, neither SDSCI nor SDSPT2 is size consistent. However, the errors can readily be cured¹⁴⁷ by us-

ing the Pople correction.²⁶⁷ This is also the case for ic-MRCISD.²⁶¹ Therefore, the SDSPT2, SDSCI, and ic-MRCISD results reported here all refer to those with the Pople corrections.

3 Computational Details

The 24 radicals and their geometries in the QUEST#4 dataset¹⁴⁵ were held unchanged in the iCIPT2,^{255,256} ic-MRCISD,²⁶¹ SDSCI,^{259,260} SDSPT2,²⁶⁰ and (MS-)NEVPT2^{257,258} calculations carried out with the BDF program package²⁶⁸⁻²⁷² under the highest Abelian group symmetries. Since the aug-cc-pVTZ (AVTZ) basis sets²⁷³⁻²⁷⁵ are good enough for most of the excitation energies (with the mean deviation (MD) only of 0.02 eV from the complete basis set (CBS) limit),¹⁴⁵ they were also used here. SA-CASSCF (state-averaged complete active space self-consistent field) calculations with equal weights for all states were first carried out (see Sec.4.3 for the various active spaces). The Dyll Hamiltonian²⁷⁶ was then diagonalized within the chosen active space and used as the active part of the zeroth-order Hamiltonian H_0 in both SDSPT2 and (MS-)NEVPT2. The inactive part (H_{in}) of H_0 is composed of orbital energies for the doubly and zero occupied orbitals. They were obtained by diagonalizing the generalized Fock matrix (constructed with the state-averaged one-particle density matrix (1RDM)) within the doubly and zero occupied subspaces separately. However, such a choice of H_{in} is problematic for states dominated by Rydberg characters (more than 70%) when they were averaged equally with valence states in the SA-CASSCF calculations. The reason is very simple: Rydberg states stem from configurations very different from those of valence states. As such, it should be better to use state-specific orbital energies, that is, the doubly and zero occupied orbital energies are to be determined by the Fock matrix that is constructed with the 1RDM of each Rydberg state itself. Conceptually, the resulting state-specific orbitals should also be used when constructing the SDSPT2/MS-NEVPT2 effective Hamiltonian matrix. However, this is not only expensive due to additional integral transformations but also means that the

off-diagonal Hamiltonian matrix elements would involve two sets of non-orthogonal orbitals. Therefore, SA-CASSCF instead of state-specific orbitals were still used in such ‘state-dependent Fock’ for H_{in} .²⁴² Although it is essentially indistinguishable from the ‘state-averaged Fock’ for valence excitations²⁴², it is a must for pure Rydberg states (see Table S1 in the Supporting Information). Nevertheless, the ‘state-averaged Fock’ still performs better for states of heavily mixed valence and Rydberg characters (e.g., the 2^2B_2 , 3^2B_2 , and 4^2B_2 states of C_3H_5 are roughly 1:1 mixtures of valence and Rydberg excitations).

Since iCIPT2 samples the whole Hilbert space, the initial SA-CASSCF calculation is not really needed, although it does provide a good start for the selection procedure. Anyway, iCIPT2 can work with natural orbitals (NOs) obtained by diagonalizing the 1RDM for the selected configurations with, e.g., $C_{\min} = 7 \times 10^{-5}$. Here, C_{\min} is the single parameter involved in iCIPT2. That is, all configuration state functions with coefficients smaller in absolute value than C_{\min} will be pruned away from the variational space determined iteratively (for more details, see Ref. 256). With the fixed NOs, a series of iCIPT2 calculations can then be performed with decreasing C_{\min} , so as to approach the FCI limit ($C_{\min} = 0$) by linear fit of the iCIPT2 vs PT2 energy plot. For both the ground and excited states, the extrapolation uncertainties at the 95% confidence level were kept below 1 mHartree. Such uncertainties for the ground and excited states were then summed up as the error bars (less than 2 mHartree or 0.05 eV) for the extrapolated VEEs. The extrapolation distances, i.e., the differences between the largest iCIPT2 calculations (at $C_{\min} = 1 \times 10^{-5}$) and extrapolated values, are also provided for reference.

It should also be mentioned that the core orbitals were kept frozen in the correlation calculations.

Finally, calculations with the spin-adapted open-shell TD-DFT^{262–264} under the Tamm-Dancoff approximation (denoted as X-TDA), in conjunction with the BHandHLYP functional^{277–279} (the simplest yet reliable functional for the low-lying doublet-doublet²⁰⁰ and

doublet-quartet excitations²⁰¹ of radicals), were also performed for comparison.

4 Results and Discussion

4.1 Reference data

Ideally, well-resolved experimental data can be taken as the reference. However, for the 24 radicals considered here, only some experimental 0-0 transitions,²⁸⁰⁻²⁹¹ after correcting the geometric and vibrational effects,^{179,202,283} are available for comparison (see Table 2). Nevertheless, they are enough to verify the accuracy of iCIPT2. It can be seen from Table 2 that iCIPT2, in conjunction with the AVTZ basis sets,²⁷³⁻²⁷⁵ is indeed very accurate, except for the $2^2A_2''$ state of CH₃ and the $2^2\Sigma^+$ state of NO. It turns out that there exist substantial basis set effects for the two states.¹⁴⁵ When the AV5Z basis set²⁷³⁻²⁷⁵ is used, the errors for the two states are reduced from 0.21 and 0.25 eV to 0.04 and 0.06 eV, respectively. Not surprisingly, the iCIPT2 results are very close to those by selected CI (sCI)¹⁴⁵ since both methods are nearly exact. The deviations of the methods (UCC3, UCCSDT, UCCSDTQ, and sCI) adopted in Ref. 145 from iCIPT2 are further plotted in Fig. 2 for the 51 doublets reported therein. All these pinpoint that the iCIPT2/AVTZ VEEs for the 110 doublets and 39 quartets of the 24 radicals can be taken as a solid reference for calibrating other methods with the same basis sets.

Table 2: Experimental and theoretical vertical excitation energies (VEEs in eV) of 26 doublet states

Radical	State	Expt.	iCIPT2/AVTZ ^a	95% interval ^b	CCSDT/AVTZ ^c	sCI/AVTZ ^{a,d}	TBE/CBS ^e
C ₃ H ₅	1 ² B ₁	3.41 ^f	3.40 ± 0.02	± 0.03	3.43	-	-
BeF	2 ² Σ ⁺	6.16 ^g	6.27 ± 0.00 ^h	± 0.01	6.23	6.21 ± 0.02	-
	1 ² Π	4.14 ^g	4.15 ± 0.00	± 0.00	4.15	4.14 ± 0.01	4.13
BeH	1 ² Π	2.48 ^g	2.49 ± 0.00	± 0.00	2.49	2.49 ± 0.00	2.48
	2 ² Π	6.32 ^g	6.46 ± 0.00	± 0.00	6.45	6.46 ± 0.00	6.46
CH	1 ² Σ ⁺	3.94 ^g	3.98 ± 0.00	± 0.00	4.03	3.98 ± 0.00	3.96
	1 ² Δ	2.88 ^g	2.91 ± 0.00	± 0.00	2.94	2.91 ± 0.00	2.90
	1 ² Σ ⁻	3.26 ⁱ	3.29 ± 0.00	± 0.00	3.31	3.29 ± 0.00	3.28
CH ₃	1 ² A' ₁	5.73 ^g	5.86 ± 0.00 (5.88 ± 0.00)	± 0.00 (± 0.01)	5.86	5.85 ± 0.01	5.88
	2 ² A'' ₂	7.44 ^g	7.65 ± 0.00 (7.48 ± 0.00)	± 0.00 (± 0.01)	7.65	7.65 ± 0.01	7.48
CN	2 ² Σ ⁺	3.22 ^g	3.22 ± 0.00	± 0.00	3.25	3.22 ± 0.00	3.21
	1 ² Π	1.32 ^g	1.34 ± 0.00	± 0.00	1.38	1.34 ± 0.01	1.33
CNO	1 ² Σ ⁺	1.55 ^j	1.62 ± 0.01	± 0.00	1.71	1.61 ± 0.01	1.61
CO ⁺	2 ² Σ ⁺	5.82 ^g	5.80 ± 0.00	± 0.00	5.70	5.81 ± 0.00	5.80
	1 ² Π	3.26 ^g	3.27 ± 0.00	± 0.00	3.26	3.28 ± 0.00	3.26
F ₂ BO	1 ² A ₁	2.77 ^k	2.77 ± 0.01	± 0.04	2.78	-	-
	1 ² B ₁	0.70 ^k	0.70 ± 0.04	± 0.03	0.71	-	-
F ₂ BS	1 ² A ₁	2.91 ^l	2.95 ± 0.02	± 0.05	2.93	-	-
	1 ² B ₁	0.46 ^l	0.50 ± 0.00	± 0.04	0.48	-	-
H ₂ PS	2 ² A'	2.77 ^m	2.73 ± 0.01	± 0.01	2.75	2.72 ± 0.02	2.71
NCO	1 ² Σ ⁺	2.80 ⁿ	2.87 ± 0.01	± 0.03	2.87	2.83 ± 0.05	2.89
NO	1 ² Σ ⁺	5.92 ^g	6.11 ± 0.01 (6.05 ± 0.01)	± 0.01 (± 0.04)	6.13	6.13 ± 0.02	6.12
	2 ² Σ ⁺	7.03 ^g	7.28 ± 0.01 (7.09 ± 0.01)	± 0.00 (± 0.04)	7.29	-	[7.21]
OH	1 ² Σ ⁺	4.09 ^g	4.11 ± 0.00	± 0.00	4.12	4.10 ± 0.01	4.09
PH ₂	1 ² A ₁	2.74 ^o	2.76 ± 0.00	± 0.00	2.77	2.77 ± 0.00	2.76
C ₂ H ₃	1 ² A''	3.22 ^p	3.28 ± 0.00	± 0.01	3.31	3.26 ± 0.02	-
MD ^q			0.05		0.06	0.05	0.04
MAD ^q			0.06		0.06	0.06	0.06
SD ^q			0.09		0.10	0.08	0.08
MAX ^q			0.25		0.26	0.21	0.18

^a ±x means extrapolation distance |x|. In parentheses are the AV5Z results. ^bSum of the 95% confidence intervals of the ground and excited states. In parentheses are the AV5Z results. ^cRef. 145. ^dRef. 145. ^eRef. 145. sCI results calculated or corrected to at least AVQZ level. In brackets is the CCSDTQ/AVQZ result. ^fRefs. 179,280. ^gRefs. 202,281,282. ^h6.22 ± 0.00 eV with the AVTZ from Basis Set Exchange.²⁹² ⁱRefs. 283,284. ^jRefs. 179,285. ^kRefs. 179,286. ^lRefs. 179,287. ^mRefs. 179,288. ⁿRefs. 179,289. ^oRefs. 179,290. ^pRefs. 179,291. ^qMD: mean deviation; MAD: mean absolute deviation; SD: standard deviation; MAX: maximum deviation. Unavailable data were excluded from the analysis.

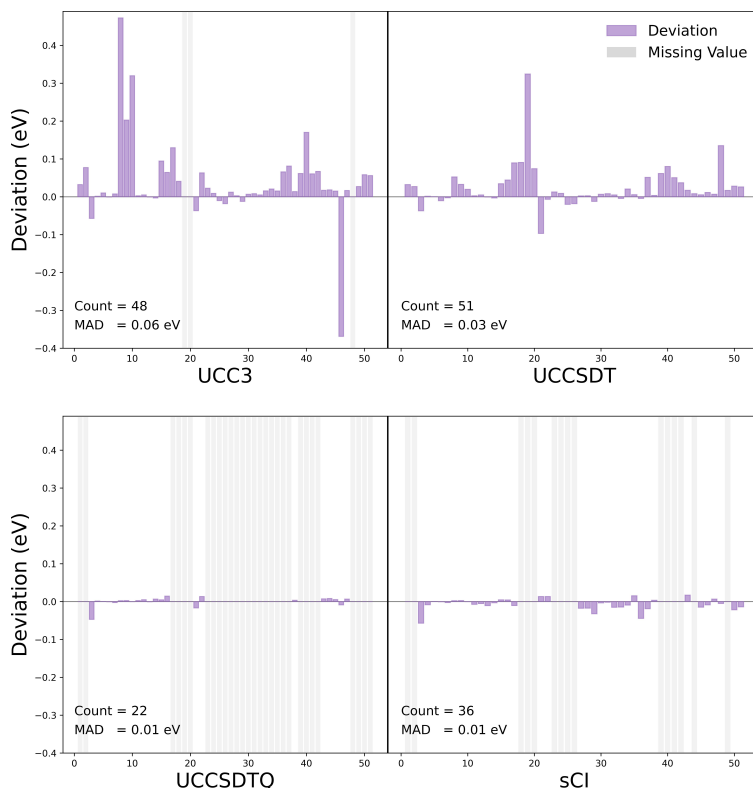


Figure 2: Deviations (in eV) of UCC3, UCCSDT, UCCSDTQ, and sCI from iCIPT2 for the 51 doublet states in QUEST#4 (AVTZ results).¹⁴⁵ Grey bars represent missing values.

4.2 QUEST#4X

Some criteria should first be established for adding additional excited states to the QUEST#4 dataset.¹⁴⁵ Since the highest VEE reported therein is 8.02 eV ($^2\Sigma^-$ of OH), only those singly excited doublet and quartet states with VEEs up to 8.0 eV are to be considered here. To identify such states, iCIPT2/AVTZ calculations were performed on the low-lying excited states of the 24 radicals for each irreducible representation (irrep). Eventually, 59 doublet states (including 17 Rydberg states) and 39 quartet states (including 6 Rydberg states) were added to QUEST#4 (which has 51 doublet states, including 11 Rydberg states), leading to QUEST#4X. Although the AVTZ basis sets may not be sufficient for some of the Rydberg states, the iCIPT2/AVTZ results can certainly be taken as the reference for calibrating other methods with the same basis sets.

4.3 Active space

Unlike iCIPT2, the NEVPT2, SDSPT2, SDSCI, and ic-MRCISD calculations all require a proper choice of active spaces. The occupation numbers (ON) of the natural orbitals (NO) resulting from the iCIPT2 calculations were taken here as guidance. Those NOs with ONs ranging from 1.98 to 0.02 were carefully analyzed as candidates for active orbitals. However, to make the MR calculations feasible, the number of active orbitals was kept below 15 (by deleting those virtual orbitals of the smallest ONs). The resulting active spaces for the 24 radicals are documented in Table 3. The SA-CASSCF calculations can be initiated and supervised by the iCAS approach (imposed automatic selection of complete active spaces),²⁹³ where once the valence atomic orbitals (see Table S2 in the Supporting Information) are prepared, all remaining steps are automated. In particular, the subspace matching algorithm therein preserves the characters of the orbitals (doubly occupied, active, or virtual) throughout the self-consistent iterations. The CASSCF energies are documented in Table S3 in the Supporting Information.

Table 3: Active spaces and electronic states by SA-CASSCF

Radical	Active Space	Symmetry	Irrep of Active MO ^a	Electronic State ^b	
				Doublet	Quartet
C ₃ H ₅	(3e,9o)	C _{2v}	(2,2,1,4)	(2,1,1,4)	(0,1,1,0)
BeF	(9e,10o)	C _{2v}	(6,0,2,2)	(2,0,1,1)	-
BeH	(3e,11o)	C _{2v}	(5,0,3,3)	(3,0,4,4)	(0,0,1,1)
BH ₂	(5e,10o)	C _{2v}	(5,0,3,2)	(3,2,2,2)	(0,1,0,0)
CH	(5e,9o)	C _{2v}	(5,0,2,2)	(3,2,1,1)	(0,1,1,1)
CH ₃	(7e,11o)	C _{2v}	(6,0,3,2)	(3,0,2,2)	-
CN	(9e,8o)	C _{2v}	(4,0,2,2)	(2,0,2,2)	(2,2,0,0)
CNO	(15e,12o)	C _{2v}	(6,0,3,3)	(3,2,3,3)	(0,0,1,1)
CON	(15e,12o)	C _{2v}	(6,0,3,3)	(1,1,2,2)	(0,0,1,1)
CO ⁺	(9e,8o)	C _{2v}	(4,0,2,2)	(2,0,1,1)	(1,0,0,0)
F ₂ BO	(19e,14o)	C _{2v}	(6,1,4,3)	(2,1,2,1)	-
F ₂ BS	(19e,14o)	C _{2v}	(6,1,4,3)	(1,0,2,1)	(0,0,1,0)
H ₂ BO	(11e,10o)	C _{2v}	(5,0,3,2)	(2,0,3,2)	(0,0,1,0)
HCO	(11e,10o)	C _s	(8,2)	(3,3)	(1,1)
HOC	(11e,10o)	C _s	(8,2)	(3,3)	(1,1)
H ₂ PO	(13e,10o)	C _s	(7,3)	(4,3)	(2,1)
H ₂ PS	(13e,10o)	C _s	(7,3)	(3,2)	(3,3)
NCO	(15e,12o)	C _{2v}	(6,0,3,3)	(2,0,3,3)	(0,0,1,1)
NH ₂	(7e,10o)	C _{2v}	(5,0,3,2)	(2,0,1,2)	(0,0,0,1)
CH ₂ NO ₂	(13e,10o)	C _{2v}	(3,1,3,3)	(2,2,2,2)	(1,1,1,0)
NO	(11e,10o)	C _{2v}	(6,0,2,2)	(2,0,2,2)	(0,1,1,1)
OH	(7e,9o)	C _{2v}	(5,0,2,2)	(1,1,1,1)	(0,1,0,0)
PH ₂	(7e,10o)	C _{2v}	(5,0,3,2)	(2,1,2,2)	(0,1,0,1)
C ₂ H ₃	(11e,12o)	C _s	(10,2)	(3,3)	(1,1)

^a C_s: (a', a''); C_{2v}: (a₁, a₂, b₂, b₁). ^b C_s: (A', A''); C_{2v}: (A₁, A₂, B₂, B₁).

4.4 Vertical Excitation Energies

The SS-NEVPT2, MS-NEVPT2, SDSPT2, SDSCI, and ic-MRCISD calculations on the VEEs of the 110 doublet and 39 quartet states of the 24 radicals in QUEST#4¹⁴⁵ were performed with the above setup of active spaces. The so-calculated VEEs are documented in Table 4. Apart from the overall error analysis shown in Table 5, the internal consistency of the methods is also analyzed in Table 6. Scatter plots for the iCIPT2 and X-TDA/SS-

NEVPT2/MS-NEVPT2/SDSPT2/SDSCI/ic-MRCISD VEEs are further depicted in Fig. 3.

It can be seen from Fig. 3 that the three variants of MRPT2 (i.e., SS-NEVPT2, MS-NEVPT2, and SDSPT2) have a strong linear correlation with iCIPT2, with R^2 larger than 0.995, which is accompanied by a mean absolute deviation (MAD) of ca. 0.1 eV. As can be seen from Table 6, the VEEs calculated by the three MRPT2 are closely aligned for more than 80% of the excited states, with the differences in between being less than 0.05 eV. However, SS-NEVPT2 fails occasionally. For instance, it fails to reproduce the ordering of the $2^2A''$ (6.83 eV) and $3^2A''$ (6.71 eV) states of H_2PO . Despite some overestimates, both MS-NEVPT2 and SDSPT2 reproduce the correct ordering for the two states (MS-NEVPT2: 6.61 and 7.04 eV; SDSPT2: 6.64 and 7.05 eV), as compared to the iCIPT2 results (6.20 and 6.81 eV). A similar situation occurs also to $1^2E'$ (2^2A_1 and 1^2B_2 under C_{2v}) and $2^2E'$ (3^2A_1 and 2^2B_2 under C_{2v}) states of CH_3 . These represent examples where dynamic correlation revises significantly the coefficients of the reference functions, as shown in Table 7. Here, it deserves to be emphasized that, although MS-NEVPT2 and SDSPT2 are hardly distinguishable for the systems considered here (see Table 6), SDSPT2 does outperform MS-NEVPT2 for situations with multiple near-degenerate states.²⁶⁰

Both SDSCI and ic-MRCISD have a perfect linear correlation with iCIPT2, with R^2 being ca. 0.999, which is accompanied by a MAD of ca. 0.05 eV. SDSCI agrees with ic-MRCISD within 0.15 eV for all the excited states, given that the computational cost of SDSCI is merely that of one iteration of ic-MRCISD. More specifically, SDSCI agrees with ic-MRCISD within 0.05, 0.10, and 0.15 eV for 75%, 95%, and 100% of the excited states, respectively (cf. Table 6). In particular, this is not fortuitous but holds also for other systems.¹⁴⁷ However, it deserves to be pointed out that both SDSCI and ic-MRCISD perform worse than the three MRPT2 for the 2^2B_2 state of nitromethyl (CH_2NO_2), see Table 4.

Compared to the above MR methods, X-TDA/BHandHLYP has a weaker linear correlation with iCIPT2, as reflected by a lower R^2 of ca. 0.927. Moreover, the orderings

of several states of BH_2 , CH_3 , H_2PO , H_2PS , and C_2H_3 were not reproduced correctly, as marked in Table 4. Nonetheless, the accuracy of X-TDA for doublet and quartet excited states of radicals is comparable to that of TD-DFT for singlet and triplet excited states of closed-shell systems, as already noticed before.^{200,201}

Having discussed the general trends, we now focus on the allyl radical C_3H_5 , which has been investigated extensively both experimentally^{280,294-297} and theoretically,²⁹⁸⁻³⁰² due to its pivotal role in photochemical reactions. It can be seen from Table 8 that seven of the nine excited states are Rydberg states. Because of this, the very first point is the proper choice of basis sets with diffuse functions,²⁹⁸⁻³⁰¹ among which the augmentation of AVTZ with molecule-centered functions (mcf)²⁹⁹ is arguably most sophisticated. As can be seen from Table 8, there does exist substantial basis set effects for the higher-lying Rydberg states (-0.49 eV for $3\ ^2B_1$ and -1.44 eV for $4\ ^2B_1$), as revealed by the UCCSD calculations.²⁹⁹ It can hence be deduced that the substantial differences (0.33 and 1.01 eV) between iCIPT2 (6.53 and 7.80 eV) and ROCC3 (6.20 and 6.79 eV)²⁹⁹ for the two states stem from the deficit of the AVTZ basis set employed here. However, the difference (-0.17 eV) between iCIPT2 (5.98 eV) and ROCC3 (6.15 eV)²⁹⁹ for the $1\ ^4A_2$ state cannot simply be ascribed to basis set effect, for ROCC3 suffers from noticeable spin contamination in this case. As for the lowest five doublet states, iCIPT2 agrees with ROCC3²⁹⁹ within 0.05 eV. On the other hand, the present ic-MRCISD results differ from the iCIPT2 ones by less than 0.15 eV for all the states. In contrast, the previous second-order MRCI³⁰⁰ or ic-MRCISD³⁰¹ results are lower than the present ic-MRCISD (iCIPT2) ones by up to 0.2 (0.3) eV. This should be ascribed to the use of a smaller basis set (DZP vs AVTZ) and a smaller active space [CAS(3e,7o) vs CAS(3e,9o)] in those calculations.

As for the MRPT2 calculations, it is first noted that, although SS-NEVPT2 predicts correctly the relative ordering of the four 2B_1 states, it overestimates the excitation energies of the $2\ ^2B_1$ and $3\ ^2B_1$ states by 0.41 eV and 0.47 eV, respectively, but underestimates that of $4\ ^2B_1$ by 0.64 eV. To understand such failures of standard MRPT2, we analyzed the wave-

functions in detail. As can be seen from Table 9, the four 2B_1 states stem primarily from four transitions, two valence and two Rydberg transitions. For the $1\ {}^2B_1$ state, which is predominantly a mixture of the two valence transitions, all MR methods yield similar results, with deviations from iCIPT2 by no more than 0.15 eV. In contrast, the wavefunctions of the other three 2B_1 states are more complex. At the CASSCF level, both $2\ {}^2B_1$ and $3\ {}^2B_1$ are dominated by Rydberg characters (>70%), while $4\ {}^2B_1$ is more akin to a valence state yet mixed with 32% Rydberg character. The situation changes dramatically at the SDSCI and ic-MRCISD levels, where these states exhibit a strong mixing of all the four components, resulting in comparable Rydberg characters exceeding 50% for each state. Such revisions of the reference states cannot be captured by standard MRPT2 like SS-NEVPT2, but can be captured to some extents by their multi-state/quasi-degenerate variants. For instance, SDSPT2 reproduces essentially all the features of SDSCI/ic-MRCISD, whereas MS-NEVPT2 is much less successful, in the sense that its $2\ {}^2B_1$ state contains only 25% Rydberg component, less than half of that of ic-MRCISD. Nevertheless, there is no significant difference in the overall accuracy of MS-NEVPT2 and SDSPT2: compared with iCIPT2, MS-NEVPT2 overestimates the excitation energies of the $2\ {}^2B_1$ to $4\ {}^2B_1$ states by 0.07, 0.12, and 0.07 eV, respectively, while SDSPT2 exhibits deviations of 0.22, 0.15, and -0.07 eV, respectively. It appears that MS-CASPT2 also performs well for these states.²⁹⁸

Table 4: Deviations (in eV) of X-TDA, SS-NEVPT2, MS-NEVPT2, SDSPT2, SDSCI, and ic-MRCISD from iCIPT2 for the vertical excitation energies (VEE) of 110 doublet and 39 quartet states

Radical	State	X-TDA	SS-NEVPT2	MS-NEVPT2	SDSPT2	SDSCI	ic-MRCISD	iCIPT2 ^a	95% interval ^b
Allyl (C ₃ H ₅)	$1\ {}^2A_1$	-0.24	0.19	0.19	0.16	-0.15	-0.06	4.94 ± 0.04	± 0.03
	$2\ {}^2A_1$	-0.28	0.24	0.24	0.21	-0.11	-0.03	5.46 ± 0.06	± 0.03
	$1\ {}^2B_2$	-0.36	0.18	0.18	0.16	-0.17	-0.08	5.61 ± 0.01	± 0.03
	$1\ {}^2B_1$	0.07	0.16	0.15	0.10	-0.13	-0.05	3.40 ± 0.02	± 0.03
	$2\ {}^2B_1$	-0.39	0.41	0.07	0.22	0.03	0.08	5.71 ± 0.05	± 0.02
	$3\ {}^2B_1$	-0.60	0.47	0.12	0.15	0.07	0.07	6.53 ± 0.01	± 0.03
	$4\ {}^2B_1$	-1.52	-0.64	0.07	-0.07	-0.08	-0.11	7.80 ± 0.02	± 0.04

Table 4: continued

Radical	State	X-TDA	SS-NEVPT2	MS-NEVPT2	SDSPT2	SDSCI	ic-MRCISD	iCIPT2 ^a	95% interval ^b	
BeF ^c	1 ⁴ A ₂	-0.31	0.22	0.22	0.19	-0.25	-0.12	5.98 ± 0.02	± 0.02	
	1 ⁴ B ₂	-0.50	0.24	0.24	0.21	-0.27	-0.14	7.68 ± 0.02	± 0.02	
	2 ² Σ ⁺	-0.33	0.01	0.01	0.01	-0.03	-0.03	6.27 ± 0.00	± 0.01	
	1 ² Π	0.05	0.02	0.02	0.04	0.06	0.03	4.15 ± 0.00	± 0.00	
BeH ^c	2 ² Σ ⁺	-0.37	0.01	0.01	0.01	0.01	0.00	5.52 ± 0.00	± 0.00	
	3 ² Σ ⁺	0.45	0.19	0.19	0.19	0.14	0.00	5.72 ± 0.00	± 0.00	
	1 ² Π	0.08	0.03	0.03	0.03	0.01	0.00	2.49 ± 0.00	± 0.00	
	2 ² Π	-0.76	0.00	0.00	0.01	0.01	0.00	6.46 ± 0.00	± 0.00	
BH ₂	3 ² Π	0.44	0.24	0.23	0.23	0.16	0.01	7.34 ± 0.00	± 0.00	
	4 ² Π	0.12	0.19	0.20	0.21	0.11	-0.03	7.80 ± 0.00	± 0.00	
	1 ⁴ Π	0.24	0.03	0.03	0.03	-0.01	0.00	5.88 ± 0.00	± 0.00	
	2 ² A ₁	-0.24	-0.03	-0.02	-0.02	-0.01	0.01	5.72 ± 0.00	± 0.00	
	3 ² A ₁	-0.35	-0.04	-0.03	-0.03	-0.02	0.01	6.75 ± 0.00	± 0.00	
	1 ² A ₂	0.17	-0.03	-0.02	-0.02	0.00	0.01	6.41 ± 0.00	± 0.00	
	2 ² A ₂	0.08	0.06	0.06	0.06	0.04	-0.03	6.95 ± 0.00	± 0.00	
	1 ² B ₂	0.19 ^d	0.05	0.05	0.06	0.04	0.00	6.38 ± 0.00	± 0.00	
	2 ² B ₂	-0.40 ^d	-0.04	-0.03	-0.04	-0.03	0.00	6.58 ± 0.00	± 0.00	
	1 ² B ₁	0.12	0.00	0.00	0.00	0.00	0.01	1.18 ± 0.00	± 0.00	
CH	2 ² B ₁	-0.37	-0.06	-0.05	-0.05	-0.02	0.01	6.87 ± 0.00	± 0.00	
	1 ⁴ A ₂	0.19	-0.03	-0.02	-0.02	0.00	0.01	5.35 ± 0.00	± 0.00	
	1 ² Σ ⁺	-1.05	0.06	0.05	0.05	0.02	0.00	3.98 ± 0.00	± 0.00	
	2 ² Σ ⁺	-0.10	-0.02	-0.02	-0.02	-0.01	-0.01	6.49 ± 0.00	± 0.00	
	1 ² Δ	0.47	0.03	0.03	0.03	0.01	-0.01	2.91 ± 0.00	± 0.00	
	1 ² Σ ⁻	0.10	0.02	0.02	0.03	0.01	-0.01	3.29 ± 0.00	± 0.00	
	1 ⁴ Σ ⁻	0.11	-0.03	-0.03	-0.04	-0.01	0.01	0.72 ± 0.00	± 0.00	
	1 ⁴ Π	-0.18	0.03	0.03	0.02	0.00	0.00	7.66 ± 0.00	± 0.00	
	CH ₃	1 ² A' ₁	-0.23	-0.02	-0.01	-0.02	-0.02	0.01	5.86 ± 0.00	± 0.00
		1 ² E'	0.04 ^d	0.17 ^d	0.07	0.09	0.11	0.04	6.96 ± 0.00	± 0.00
2 ² E'		-0.45 ^d	-0.14 ^d	-0.01	-0.05	-0.05	-0.03	7.19 ± 0.00	± 0.00	
CN	2 ² A'' ₂	-0.26	-0.06	-0.03	-0.03	-0.01	0.00	7.65 ± 0.00	± 0.00	
	2 ² Σ ⁺	0.36	0.02	0.04	0.05	0.02	-0.01	3.22 ± 0.00	± 0.00	
	1 ² Π	-0.46	0.04	0.05	0.05	0.00	-0.01	1.34 ± 0.00	± 0.00	
	2 ² Π	0.84	0.11	0.12	0.14	0.07	0.01	7.88 ± 0.00	± 0.00	
	1 ⁴ Σ ⁺	-0.30	0.04	0.05	0.05	0.02	0.02	6.03 ± 0.00	± 0.00	
CNO	1 ⁴ Δ	-0.70	0.07	0.08	0.09	0.03	0.00	7.12 ± 0.00	± 0.00	
	1 ⁴ Σ ⁻	-0.74	0.13	0.14	0.15	0.05	0.01	7.88 ± 0.00	± 0.00	
	1 ² Σ ⁺	1.49	-0.08	-0.08	-0.08	0.05	0.01	1.62 ± 0.01	± 0.00	
	2 ² Σ ⁺	0.33	0.10	0.11	0.11	0.06	0.08	7.63 ± 0.03	± 0.01	

Table 4: continued

Radical	State	X-TDA	SS-NEVPT2	MS-NEVPT2	SDSPT2	SDSCI	ic-MRCISD	iCIPT2 ^a	95% interval ^b
CON	1 ² Δ	0.75	0.10	0.11	0.13	0.12	0.07	7.69 ± 0.02	± 0.01
	1 ² Σ ⁻	-0.43	-0.19	-0.18	-0.16	-0.18	-0.18	7.82 ± 0.02	± 0.01
	2 ² Π	0.31	0.04	0.05	0.05	0.02	0.02	5.48 ± 0.01	± 0.00
	3 ² Π	0.00	0.09	0.10	0.11	0.05	0.06	6.18 ± 0.03	± 0.01
	1 ⁴ Π	0.08	0.07	0.08	0.09	0.04	0.06	5.70 ± 0.01	± 0.00
	1 ² Σ ⁺	2.42	-0.04	-0.04	-0.04	0.03	0.00	3.80 ± 0.02	± 0.01
	1 ² Σ ⁻	-0.47	0.04	0.04	0.07	0.07	0.05	7.15 ± 0.02	± 0.01
	2 ² Π	-0.08	0.04	0.04	0.05	0.05	0.05	3.47 ± 0.01	± 0.00
CO ⁺	1 ⁴ Π	-0.20	-0.03	-0.03	-0.01	0.01	0.02	2.74 ± 0.00	± 0.00
	2 ² Σ ⁺	0.83	0.05	0.05	0.07	0.01	-0.01	5.80 ± 0.00	± 0.00
	1 ² Π	0.10	0.03	0.04	0.05	-0.01	0.00	3.27 ± 0.00	± 0.00
	1 ⁴ Σ ⁺	-0.27	0.06	0.07	0.08	0.02	0.01	7.27 ± 0.00	± 0.00
F ₂ BO	1 ² A ₁	0.15	0.04	0.04	0.04	0.01	0.01	2.77 ± 0.01	± 0.04
	2 ² A ₁	1.25	0.21	0.21	0.23	0.04	0.11	7.79 ± 0.12	± 0.04
	1 ² A ₂	1.23	0.21	0.21	0.22	-0.04	0.07	6.94 ± 0.07	± 0.03
	2 ² B ₂	1.37	0.26	0.26	0.27	-0.02	0.08	6.53 ± 0.11	± 0.03
	1 ² B ₁	0.07	-0.01	-0.01	-0.01	-0.01	0.00	0.70 ± 0.04	± 0.03
F ₂ BS	1 ² A ₁	0.09	0.09	0.09	0.10	-0.01	0.04	2.95 ± 0.02	± 0.05
	2 ² B ₂	0.09	0.08	0.08	0.10	0.16	0.12	7.02 ± 0.05	± 0.04
	1 ² B ₁	-0.04	0.05	0.05	0.05	-0.01	-0.02	0.50 ± 0.00	± 0.04
	1 ⁴ B ₂	-0.03	-0.04	-0.04	-0.03	0.08	0.05	6.39 ± 0.03	± 0.05
H ₂ BO	1 ² A ₁	0.02	0.06	0.06	0.07	0.01	0.00	3.51 ± 0.00	± 0.01
	2 ² A ₁	1.16	0.06	0.07	0.09	0.07	0.04	7.25 ± 0.00	± 0.01
	2 ² B ₂	1.03	0.00	0.00	0.00	0.04	0.02	4.61 ± 0.00	± 0.01
	3 ² B ₂	1.09	0.05	0.06	0.08	0.00	0.03	7.64 ± 0.00	± 0.01
	1 ² B ₁	-0.21	0.04	0.04	0.05	-0.02	0.00	2.17 ± 0.00	± 0.01
HCO	2 ² B ₁	0.98	0.08	0.08	0.11	0.07	0.05	6.13 ± 0.01	± 0.01
	1 ⁴ B ₂	0.73	0.07	0.07	0.09	0.00	0.05	6.86 ± 0.00	± 0.01
	2 ² A'	0.24	0.17	0.17	0.17	-0.05	0.03	5.45 ± 0.01	± 0.01
	3 ² A'	0.07	0.17	0.18	0.18	0.07	0.08	6.15 ± 0.01	± 0.01
	1 ² A''	0.17	-0.01	-0.02	0.00	0.04	0.02	2.09 ± 0.00	± 0.01
	2 ² A''	-0.18	0.11	0.11	0.11	-0.02	0.01	7.07 ± 0.01	± 0.01
	3 ² A''	-0.28	0.08	0.10	0.11	-0.01	0.00	7.73 ± 0.01	± 0.01
	1 ⁴ A'	-0.21	0.05	0.05	0.05	-0.02	0.04	6.75 ± 0.01	± 0.01
HOC	1 ⁴ A''	-0.21	0.04	0.05	0.05	0.00	0.05	6.37 ± 0.01	± 0.01
	2 ² A'	0.36	0.14	0.14	0.13	-0.04	0.02	3.78 ± 0.00	± 0.01
	3 ² A'	0.11	0.13	0.13	0.14	0.09	0.04	5.63 ± 0.01	± 0.01
	1 ² A''	0.01	-0.01	-0.01	0.00	0.02	0.00	0.92 ± 0.00	± 0.01

Table 4: continued

Radical	State	X-TDA	SS-NEVPT2	MS-NEVPT2	SDSPT2	SDSCI	ic-MRCISD	iCIPT2 ^a	95% interval ^b	
H ₂ PO	2 ² A''	0.20	0.07	0.07	0.10	0.06	0.03	6.13 ± 0.01	± 0.01	
	3 ² A''	0.28	0.15	0.15	0.17	0.08	0.06	7.55 ± 0.01	± 0.01	
	1 ⁴ A'	0.24	0.18	0.18	0.17	-0.02	0.05	7.73 ± 0.01	± 0.01	
	1 ⁴ A''	0.05	-0.08	-0.08	-0.08	0.00	0.02	3.84 ± 0.01	± 0.01	
	2 ² A'	-0.05	0.18	0.24	0.25	0.08	0.04	4.21 ± 0.01	± 0.03	
	3 ² A'	0.41	0.08	0.18	0.20	0.06	0.05	4.78 ± 0.01	± 0.04	
	4 ² A'	-0.03	0.14	0.21	0.23	0.02	0.03	5.66 ± 0.02	± 0.02	
	1 ² A''	-0.01	0.11	0.17	0.16	-0.04	0.01	2.81 ± 0.01	± 0.03	
	2 ² A''	0.37	0.63 ^d	0.41	0.44	0.30	0.21	6.20 ± 0.02	± 0.04	
	3 ² A''	0.65	-0.11 ^d	0.23	0.23	-0.04	0.05	6.81 ± 0.03	± 0.03	
H ₂ PS	1 ⁴ A'	0.06	0.18	0.24	0.25	0.02	0.10	7.28 ± 0.02	± 0.03	
	2 ⁴ A'	0.57	0.27	0.32	0.32	0.10	0.18	7.64 ± 0.02	± 0.03	
	1 ⁴ A''	0.53	0.16	0.22	0.23	0.02	0.12	6.31 ± 0.02	± 0.03	
	2 ² A'	0.13	0.09	0.11	0.11	0.04	0.02	2.73 ± 0.01	± 0.01	
	3 ² A'	0.12	0.19	0.20	0.21	0.02	0.02	4.57 ± 0.02	± 0.01	
	1 ² A''	-0.09	0.08	0.09	0.09	-0.02	0.02	1.14 ± 0.00	± 0.01	
	2 ² A''	0.59	0.12	0.13	0.14	0.04	0.09	5.42 ± 0.03	± 0.01	
	1 ⁴ A'	0.66	0.17	0.18	0.17	0.03	0.10	5.74 ± 0.01	± 0.01	
	2 ⁴ A'	0.68 ^d	0.23	0.19	0.22	0.07	0.07	6.02 ± 0.01	± 0.01	
	3 ⁴ A'	-0.76 ^d	0.34	0.40	0.40	0.15	0.17	6.76 ± 0.02	± 0.01	
NCO	1 ⁴ A''	1.09 ^d	0.21	0.19	0.20	0.10	0.10	5.08 ± 0.01	± 0.02	
	2 ⁴ A''	-0.34 ^d	0.46	0.49	0.51	0.23	0.22	5.73 ± 0.02	± 0.01	
	3 ⁴ A''	-0.05	0.14	0.16	0.16	-0.02	0.06	6.72 ± 0.01	± 0.01	
	1 ² Σ ⁺	0.22	-0.04	-0.03	-0.03	0.05	0.01	2.87 ± 0.01	± 0.03	
	2 ² Σ ⁺	1.22	0.07	0.08	0.08	0.03	0.03	7.03 ± 0.02	± 0.02	
	2 ² Π	0.88	0.03	0.05	0.05	0.02	0.02	4.72 ± 0.01	± 0.02	
	3 ² Π	0.04	0.10	0.11	0.12	0.07	0.05	7.43 ± 0.03	± 0.02	
	1 ⁴ Π	-0.12	0.06	0.07	0.08	0.04	0.06	6.79 ± 0.01	± 0.02	
	NH ₂	1 ² A ₁	0.08	0.02	0.02	0.02	0.00	0.00	2.12 ± 0.00	± 0.00
		2 ² A ₁	0.04	0.06	0.06	0.05	0.00	0.00	7.69 ± 0.00	± 0.00
1 ² B ₂		0.01	0.06	0.06	0.07	0.01	0.01	6.48 ± 0.00	± 0.00	
2 ² B ₁		0.02	0.03	0.03	0.02	-0.02	0.00	7.75 ± 0.00	± 0.00	
1 ⁴ B ₁		0.04	0.04	0.04	0.03	0.00	0.01	7.29 ± 0.00	± 0.00	
Nitromethyl (CH ₂ NO ₂)	1 ² A ₁	0.84	-0.03	0.03	-0.01	0.21	0.15	2.50 ± 0.01	± 0.03	
	2 ² A ₁	0.35	-0.05	0.01	-0.01	0.06	0.07	5.20 ± 0.01	± 0.04	
	1 ² A ₂	1.13	-0.05	-0.02	-0.04	0.10	0.08	2.30 ± 0.00	± 0.03	
	2 ² A ₂	0.64	0.03	0.13	0.15	0.11	0.15	6.70 ± 0.07	± 0.03	
	1 ² B ₂	1.02	-0.03	0.03	0.01	0.13	0.11	2.00 ± 0.02	± 0.04	

Table 4: continued

Radical	State	X-TDA	SS-NEVPT2	MS-NEVPT2	SDSPT2	SDSCI	ic-MRCISD	iCIPT2 ^a	95% interval ^b	
NO	2^2B_2	0.33	-0.02	0.04	0.02	-0.01	0.03	4.66 ± 0.02	± 0.04	
	2^2B_1	0.21	-0.05	0.08	0.13	0.42	0.30	5.31 ± 0.00	± 0.03	
	1^4A_1	0.04	0.00	0.06	0.04	0.06	0.09	4.94 ± 0.03	± 0.02	
	1^4A_2	-0.52	-0.05	0.01	-0.02	-0.05	0.00	4.30 ± 0.02	± 0.03	
	1^4B_2	0.10	0.01	0.07	0.05	0.00	0.05	4.46 ± 0.03	± 0.04	
	$1^2\Sigma^+$	0.46	0.19	0.19	0.19	-0.09	-0.01	6.11 ± 0.01	± 0.01	
	$2^2\Sigma^+$	0.28	0.17	0.17	0.16	-0.11	-0.02	7.28 ± 0.01	± 0.00	
	$2^2\Pi$	-0.45	-0.04	-0.04	-0.04	-0.15	-0.13	7.79 ± 0.00	± 0.01	
	$1^4\Sigma^-$	-0.21	-0.04	-0.04	-0.02	0.05	0.02	6.36 ± 0.00	± 0.01	
	$1^4\Pi$	-0.45	0.06	0.06	0.05	-0.03	0.02	6.78 ± 0.00	± 0.01	
OH	$1^2\Sigma^+$	0.04	0.01	0.01	0.01	0.01	0.00	4.11 ± 0.00	± 0.00	
	$1^2\Sigma^-$	0.09	0.01	0.01	0.01	-0.01	-0.01	8.03 ± 0.00	± 0.00	
	$1^4\Sigma^-$	0.09	0.02	0.02	0.02	0.00	-0.01	7.50 ± 0.00	± 0.00	
PH ₂	1^2A_1	0.05	0.07	0.07	0.07	0.04	-0.01	2.76 ± 0.00	± 0.00	
	2^2A_1	-0.15	0.05	0.05	0.04	0.00	0.02	5.90 ± 0.00	± 0.00	
	1^2A_2	0.24	0.21	0.21	0.22	0.10	0.02	7.10 ± 0.00	± 0.00	
	1^2B_2	0.08	0.10	0.10	0.10	0.03	-0.02	5.17 ± 0.00	± 0.00	
	2^2B_2	-0.07	0.08	0.09	0.09	0.02	-0.02	5.75 ± 0.00	± 0.00	
	2^2B_1	-0.14	0.06	0.06	0.06	0.01	0.01	7.47 ± 0.00	± 0.00	
	1^4A_2	0.09	0.04	0.04	0.04	0.00	0.03	6.16 ± 0.00	± 0.00	
	1^4B_1	-0.03	0.13	0.13	0.13	0.06	0.05	6.95 ± 0.00	± 0.00	
	Vinyl (C ₂ H ₃)	$2^2A'$	0.75 ^d	0.10	0.09	0.11	0.02	0.02	5.60 ± 0.00	± 0.02
		$3^2A'$	-0.80 ^d	0.13	0.17	0.15	-0.06	0.01	6.19 ± 0.01	± 0.01
$1^2A''$		-0.10	0.04	0.05	0.05	0.01	-0.03	3.28 ± 0.00	± 0.01	
$2^2A''$		-0.03	0.05	0.06	0.09	0.08	0.02	4.70 ± 0.00	± 0.01	
$3^2A''$		-0.42	0.14	0.16	0.15	-0.07	0.02	7.54 ± 0.01	± 0.01	
$1^4A'$		-0.15	0.05	0.06	0.05	-0.03	0.02	4.54 ± 0.01	± 0.01	
$1^4A''$		-0.38	0.16	0.17	0.15	-0.08	0.03	7.40 ± 0.01	± 0.01	

^a $\pm x$ means extrapolation distance $|x|$.

^b Sum of the 95% confidence intervals of ground and excited states.

^c The AVTZ basis set of Be varies across different program packages.

^d Incorrect ordering.

Table 5: Statistical analysis of the errors (in eV) of X-TDA, SS-NEVPT2, MS-NEVPT, SDSPT2, SDSCI, and ic-MRCISD relative to iCIPT2 for the vertical excitation energies of 110 doublet and 39 quartet states*

Type		X-TDA	SS-NEVPT2	MS-NEVPT2	SDSPT2	SDSCI	ic-MRCISD
Doublets (110 states)	MD	0.17	0.07	0.08	0.08	0.02	0.02
	MAD	0.40	0.10	0.09	0.10	0.06	0.04
	SD	0.58	0.15	0.12	0.12	0.08	0.06
	MAX	2.42	0.63	0.41	0.44	0.42	0.30
Quartets (39 states)	MD	-0.03	0.09	0.11	0.11	0.01	0.04
	MAD	0.31	0.11	0.12	0.12	0.05	0.06
	SD	0.41	0.15	0.16	0.16	0.08	0.08
	MAX	1.09	0.46	0.49	0.51	0.23	0.22
Overall (149 states)	MD	0.12	0.07	0.09	0.09	0.02	0.03
	MAD	0.38	0.10	0.10	0.10	0.05	0.04
	SD	0.54	0.15	0.13	0.13	0.08	0.07
	MAX	2.42	0.63	0.49	0.51	0.42	0.30

* MD: mean deviation; MAD: mean absolute deviation; SD: standard deviation; MAX: maximum deviation.

Table 6: Internal consistency (percentage number of states within a deviation range in absolute value) across SS-NEVPT2, MS-NEVPT2, SDSPT2, SDSCI, ic-MRCISD, and iCIPT2

Deviation Range (eV)	SS-NEVPT2	SS-NEVPT2	MS-NEVPT2	MS-NEVPT2	SDSPT2	SDSCI	ic-MRCISD
	vs MS-NEVPT2	vs SDSPT2	vs SDSPT2	vs SDSCI	vs SDSCI	vs ic-MRCISD	vs iCIPT2
0.05	84 %	89 %	99 %	50 %	44 %	75 %	74%
0.10	95 %	95 %	99 %	72 %	68 %	95 %	89%
0.15	97 %	96 %	100 %	82 %	81 %	100 %	96%

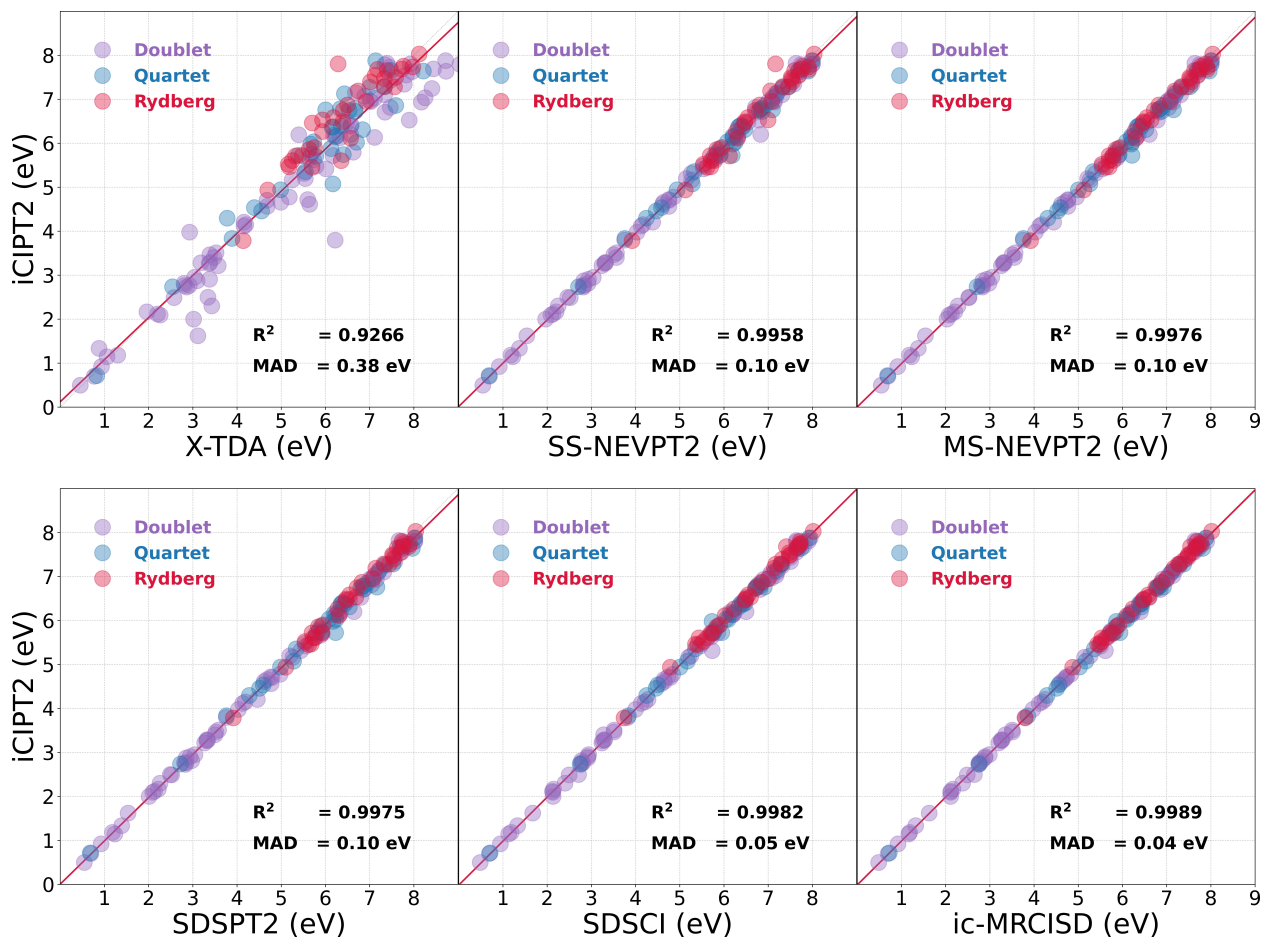


Figure 3: Scatter plots for the iCIPT2 and X-TDA/NEVPT2/SDSPT2/SDSCI/ic-MRCISD VEEs for the QUEST#4X dataset (MAD: mean absolute deviation)

Table 7: CASSCF, MS-NEVPT2, and SDSPT2 wavefunctions of excited states of H₂PO and CH₃

H ₂ PO	Ground state: (10a') ¹ (3a'') ²	
	(3a'') ² → (11a') ⁰	(10a') ¹ → (4a'') ¹
$\Psi_{2\ 2A''}^{\text{CASSCF}}$	72%	15%
$\Psi_{3\ 2A''}^{\text{CASSCF}}$	18%	62%
$\Psi_{2\ 2A''}^{\text{MS-NEVPT2}}$	3%	75%
$\Psi_{3\ 2A''}^{\text{MS-NEVPT2}}$	87%	3%
$\Psi_{2\ 2A''}^{\text{SDSPT2}}$	7%	73%
$\Psi_{3\ 2A''}^{\text{SDSPT2}}$	84%	5%

CH ₃	Ground state: (3a ₁) ² (1b ₂) ² (1b ₁) ¹	
	(1b ₁) ¹ → (5a ₁) ⁰	(3a ₁) ² → (1b ₁) ¹
$\Psi_{2\ 2A_1(1\ 2E')}^{\text{CASSCF}}$	96%	0%
$\Psi_{3\ 2A_1(2\ 2E')}^{\text{CASSCF}}$	0%	95%
$\Psi_{2\ 2A_1(1\ 2E')}^{\text{MS-NEVPT2}}$	20%	76%
$\Psi_{3\ 2A_1(2\ 2E')}^{\text{MS-NEVPT2}}$	75%	20%
$\Psi_{2\ 2A_1(1\ 2E')}^{\text{SDSPT2}}$	42%	54%
$\Psi_{3\ 2A_1(2\ 2E')}^{\text{SDSPT2}}$	54%	41%
	(1b ₁) ¹ → (2b ₂) ⁰	(1b ₂) ² → (1b ₁) ¹
$\Psi_{1\ 2B_2(1\ 2E')}^{\text{CASSCF}}$	96%	0%
$\Psi_{2\ 2B_2(2\ 2E')}^{\text{CASSCF}}$	0%	95%
$\Psi_{1\ 2B_2(1\ 2E')}^{\text{MS-NEVPT2}}$	20%	76%
$\Psi_{2\ 2B_2(2\ 2E')}^{\text{MS-NEVPT2}}$	75%	20%
$\Psi_{1\ 2B_2(1\ 2E')}^{\text{SDSPT2}}$	48%	48%
$\Psi_{2\ 2B_2(2\ 2E')}^{\text{SDSPT2}}$	48%	47%

Table 8: Vertical excitation energies (in eV) of C₃H₅

Type ^a		SS-NEVPT2 AVTZ	MS-NEVPT2 AVTZ	SDSPT2 AVTZ	SDSCI AVTZ	ic-MRCISD AVTZ	iCIPT2 ^b AVTZ	95% interval ^c
1 ² B ₁	Val.	3.57	3.56	3.50	3.28	3.36	3.40 ± 0.02	± 0.03
1 ² A ₁	Ryd.	5.13	5.13	5.10	4.79	4.87	4.94 ± 0.04	± 0.03
2 ² A ₁	Ryd.	5.70	5.70	5.68	5.35	5.44	5.46 ± 0.06	± 0.03
1 ² B ₂	Ryd.	5.79	5.79	5.77	5.43	5.53	5.61 ± 0.01	± 0.03
2 ² B ₁	Ryd.	6.12	5.78	5.93	5.74	5.79	5.71 ± 0.05	± 0.02
1 ⁴ A ₂	Val.	6.20	6.20	6.17	5.73	5.86	5.98 ± 0.02	± 0.02
3 ² B ₁	Ryd.	7.00	6.65	6.68	6.60	6.60	6.53 ± 0.01	± 0.03
1 ⁴ B ₂	Ryd.	7.92	7.92	7.89	7.41	7.54	7.68 ± 0.02	± 0.02
4 ² B ₁	Ryd.	7.17	7.87	7.73	7.72	7.69	7.80 ± 0.02	± 0.04

Type ^a		CI2 ^d DZP + 2s1p on C	ic-MRCISD ^e DZP + 1s1p on C	MS-CASPT2 ^f ANO-L + 1s1p1d on C	ROCC3 ^h AVTZ + mcf: 2s2p2d	mcf effect ⁱ of UCCSD	iCIPT2 ^b AVTZ	95% interval ^c
1 ² B ₁	Val.	3.36	3.32	3.32	3.44	0.03	3.40 ± 0.02	± 0.03
1 ² A ₁	Ryd.	4.70	4.68	5.11	4.94	-0.01	4.94 ± 0.04	± 0.03
2 ² A ₁	Ryd.	5.25	5.25	5.65	5.49	-0.02	5.46 ± 0.06	± 0.03
1 ² B ₂	Ryd.	5.31	5.29	5.76	5.59	0.09	5.61 ± 0.01	± 0.03
2 ² B ₁	Ryd.	5.50	5.46	5.73	5.65	-0.09	5.71 ± 0.05	± 0.02
1 ⁴ A ₂	Val.	-	-	5.89 ^g	6.15	0.04	5.98 ± 0.02	± 0.02
3 ² B ₁	Ryd.	-	-	6.36	6.20	-0.49	6.53 ± 0.01	± 0.03
1 ⁴ B ₂	Ryd.	-	-	-	-	-	7.68 ± 0.02	± 0.02
4 ² B ₁	Ryd.	-	-	6.90	6.79	-1.44	7.80 ± 0.02	± 0.04

^a Val.: valence excitation; Ryd.: Rydberg excitation.

^b ±*x* means extrapolation distance $|x|$.

^c Sum of the 95% confidence intervals of ground and excited states.

^d Ref. 300; second-order MRCI with (3e,7o).

^e Ref. 301; ic-MRCISD with (3e,7o).

^f Ref. 298; ANO-L: C(14s9p4d)/H(8s4p) → C[4s3p2d]/H[3s2p]; (3e,7o) for the doublets, whereas (3e,3o) for 1⁴A₂.

^g Ref. 298; CASPT2 with (3e,3o).

^h Ref. 299; mcf: molecule-centered basis functions.

ⁱ Ref. 299; E(UCCSD/AVTZ + mcf) – E(UCCSD/AVTZ).

Table 9: CASSCF, MS-NEVPT2, SDSPT2, SDSCI, and ic-MRCISD wavefunctions of excited states of C_3H_5

C_3H_5	Ground state: $(6a_1)^2(1a_2)^1(4b_2)^2(1b_1)^2$				
	$(1a_2)^1 \rightarrow (2b_1)^0$	$(1b_1)^2 \rightarrow (1a_2)^1$	$(1a_2)^1 \rightarrow (3b_1)^0$	$(1a_2)^1 \rightarrow (4b_1)^0$	Rydberg
	Valence	Valence	Rydberg	Rydberg	component
$\Psi_{1\ 2B_1}^{CASSCF}$	41%	49%	1%	0%	1%
$\Psi_{2\ 2B_1}^{CASSCF}$	10%	5%	51%	28%	79%
$\Psi_{3\ 2B_1}^{CASSCF}$	8%	11%	41%	33%	74%
$\Psi_{4\ 2B_1}^{CASSCF}$	29%	25%	0%	32%	32%
$\Psi_{1\ 2B_1}^{MS-NEVPT2}$	43%	48%	0%	0%	0%
$\Psi_{2\ 2B_1}^{MS-NEVPT2}$	37%	30%	11%	14%	25%
$\Psi_{3\ 2B_1}^{MS-NEVPT2}$	6%	10%	71%	3%	74%
$\Psi_{4\ 2B_1}^{MS-NEVPT2}$	2%	3%	10%	76%	86%
$\Psi_{1\ 2B_1}^{SDSPT2}$	41%	49%	0%	0%	0%
$\Psi_{2\ 2B_1}^{SDSPT2}$	21%	13%	34%	26%	60%
$\Psi_{3\ 2B_1}^{SDSPT2}$	14%	17%	55%	4%	59%
$\Psi_{4\ 2B_1}^{SDSPT2}$	11%	12%	3%	63%	66%
$\Psi_{1\ 2B_1}^{SDSCI}$	40%	51%	0%	0%	0%
$\Psi_{2\ 2B_1}^{SDSCI}$	18%	9%	39%	28%	67%
$\Psi_{3\ 2B_1}^{SDSCI}$	14%	15%	52%	11%	63%
$\Psi_{4\ 2B_1}^{SDSCI}$	17%	16%	2%	54%	56%
$\Psi_{1\ 2B_1}^{ic-MRCISD}$	36%	45%	0%	0%	0%
$\Psi_{2\ 2B_1}^{ic-MRCISD}$	18%	11%	32%	23%	55%
$\Psi_{3\ 2B_1}^{ic-MRCISD}$	13%	15%	48%	5%	53%
$\Psi_{4\ 2B_1}^{ic-MRCISD}$	11%	11%	3%	55%	58%

5 Conclusions

A comprehensive dataset, QUEST#4X, has been introduced for the purpose of calibrating multireference (MR) methods. It encompasses 110 doublet and 39 quartet excited states for the 24 radicals in the dataset QUEST#4 (which has only 51 doublet states). The iCIPT2/AVTZ vertical excitation energies reported here serve as a benchmark for any other MR methods. It is of interest to note that the MR methods considered here, i.e., NEVPT2, SDSPT2, SDSCI, and ic-MRCISD, share the same function space and differ only

in the determination of the expansion coefficients. Because of this, SDSCI can be taken as the initial step of ic-MRCISD and can even yield SDSPT2 and MS-NEVPT2 results automatically. Moreover, SDSPT2 also yields MS-NEVPT2 results automatically. More interestingly, the degree of agreement between SDSPT2 and MS-NEVPT2, the magnitude of deviations of SDSPT2/MS-NEVPT2 from SDSCI, as well as the iterative increments going from SDSCI to ic-MRCISD are clear indicators for the internal consistency between the methods and hence their accuracy. A good internal consistency can only be achieved by choosing appropriate active spaces for all target states, as done here. Notwithstanding this, more challenging datasets for the excited states of open-shell transition metals and *f*-elements remain to be established. Work along this direction is being carried out at our laboratory.

Acknowledgments

This work was supported by the National Natural Science Foundation of China (Grant No. 22373057) and Mount Tai Scholar Climbing Project of Shandong Province.

Supporting Information

Information for the radicals under concern, proper choice of zeroth-order Hamiltonian for Rydberg states, valence atomic orbitals, and CASSCF energies.

Conflicts of interest

There are no conflicts to declare.

References

- (1) Marenich, A. V.; Jerome, S. V.; Cramer, C. J.; Truhlar, D. G. Charge Model 5: An Extension of Hirshfeld Population Analysis for the Accurate Description of Molecular Interactions in Gaseous and Condensed Phases. *J. Chem. Theory Comput.* **2012**, *8*, 527–541.
- (2) Verma, P.; Truhlar, D. G. Can Kohn–Sham density functional theory predict accurate charge distributions for both single-reference and multi-reference molecules? *Phys. Chem. Chem. Phys.* **2017**, *19*, 12898–12912.
- (3) Grimme, S. Semiempirical Hybrid Density Functional with Perturbative Second-order Correlation. *J. Chem. Phys.* **2006**, *124*, 034108.
- (4) Zhao, Y.; Truhlar, D. G. The M06 Suite of Density Functionals for Main Group Thermochemistry, Thermochemical Kinetics, Noncovalent Interactions, Excited States, and Transition Elements: Two New Functionals and Systematic Testing of Four M06-class Functionals and 12 Other Functionals. *Theor. Chem. Acc* **2008**, *120*, 215–241.
- (5) Peverati, R.; Truhlar, D. G. Quest for a Universal Density Functional: the Accuracy of Density Functionals Across a Broad Spectrum of Databases in Chemistry and Physics. *Philos. Trans. Royal Soc. A* **2014**, *372*, 20120476, Article 20120476.
- (6) Haoyu, S. Y.; Zhang, W.; Verma, P.; He, X.; Truhlar, D. G. Nonseparable Exchange–Correlation Functional for Molecules, Including Homogeneous Catalysis Involving Transition Metals. *Phys. Chem. Chem. Phys.* **2015**, *17*, 12146–12160.
- (7) Verma, P.; Wang, Y.; Ghosh, S.; He, X.; Truhlar, D. G. Revised M11 Exchange–correlation Functional for Electronic Excitation Energies and Ground-State Properties. *J. Phys. Chem. A* **2019**, *123*, 2966–2990.

- (8) Liu, Y.; Zhang, C.; Liu, Z.; Truhlar, D. G.; Wang, Y.; He, X. Supervised Learning of a Chemistry Functional with Damped Dispersion. *Nat. Comput. Sci.* **2023**, *3*, 48–58.
- (9) Goerigk, L.; Grimme, S. A General Database for Main Group Thermochemistry, Kinetics, and Noncovalent Interactions – Assessment of Common and Reparameterized (meta-) GGA Density Functionals. *J. Chem. Theory Comput.* **2010**, *6*, 107–126.
- (10) Goerigk, L.; Grimme, S. Efficient and Accurate Double-Hybrid-Meta-GGA Density Functionals-Evaluation with the Extended GMTKN30 Database for General Main Group Thermochemistry, Kinetics, and Noncovalent Interactions. *J. Chem. Theory Comput.* **2011**, *7*, 291–309.
- (11) Goerigk, L.; Hansen, A.; Bauer, C.; Ehrlich, S.; Najibi, A.; Grimme, S. A Look at the Density Functional Theory Zoo with the Advanced GMTKN55 Database for General Main Group Thermochemistry, Kinetics, and Noncovalent Interactions. *Phys. Chem. Chem. Phys.* **2017**, *19*, 32184–32215.
- (12) Mardirossian, N.; Head-Gordon, M. How Accurate Are the Minnesota Density Functionals for Noncovalent Interactions, Isomerization Energies, Thermochemistry, and Barrier Heights Involving Molecules Composed of Main-Group Elements? *J. Chem. Theory Comput.* **2016**, *12*, 4303–4325.
- (13) Yu, H.; Truhlar, D. G. Components of the Bond Energy in Polar Diatomic Molecules, Radicals, and Ions Formed by Group-1 and Group-2 Metal Atoms. *J. Chem. Theory Comput.* **2015**, *11*, 2968–2983.
- (14) Zhao, Y.; González-García, N.; Truhlar, D. G. Benchmark Database of Barrier Heights for Heavy Atom Transfer, Nucleophilic Substitution, Association, and Unimolecular Reactions and Its Use to Test Theoretical Methods. *J. Phys. Chem. A* **2005**, *109*, 2012–2018.

- (15) Curtiss, L. A.; Redfern, P. C.; Raghavachari, K.; Pople, J. A. Assessment of Gaussian-2 and Density Functional Theories for the Computation of Ionization Potentials and Electron Affinities. *J. Chem. Phys.* **1998**, *109*, 42–55.
- (16) Karton, A.; Daon, S.; Martin, J. M. L. W4-11: A High-confidence Benchmark Dataset for Computational Thermochemistry Derived From First-principles W4 Data. *Chem. Phys. Lett.* **2011**, *510*, 165–178.
- (17) Xu, X.; Alecu, I. M.; Truhlar, D. G. How Well Can Modern Density Functionals Predict Internuclear Distances at Transition States? *J. Chem. Theory Comput.* **2011**, *7*, 1667–1676.
- (18) Zhao, Y.; Ng, H. T.; Peverati, R.; Truhlar, D. G. Benchmark Database for Ylidic Bond Dissociation Energies and Its Use for Assessments of Electronic Structure Methods. *J. Chem. Theory Comput.* **2012**, *8*, 2824–2834.
- (19) Pople, J. A.; Head-Gordon, M.; Fox, D. J.; Raghavachari, K.; Curtiss, L. A. Gaussian-1 Theory: A General Procedure for Prediction of Molecular Energies. *J. Chem. Phys.* **1989**, *90*, 5622–5629.
- (20) Curtiss, L. A.; Raghavachari, K.; Trucks, G. W.; Pople, J. A. Gaussian-2 Theory for Molecular Energies of First- and Second-Row Compounds. *J. Chem. Phys.* **1991**, *94*, 7221–7230.
- (21) O'Reilly, R. J.; Karton, A. A Dataset of Highly Accurate Homolytic N-Br Bond Dissociation Energies Obtained by Means of W2 Theory. *Int. J. Quantum Chem.* **2016**, *116*, 52–60.
- (22) Cleland, D.; Booth, G. H.; Overy, C.; Alavi, A. Taming the First-Row Diatomics: A Full Configuration Interaction Quantum Monte Carlo Study. *J. Chem. Theory Comput.* **2012**, *8*, 4138–4152.

- (23) Chilkuri, V. G.; Neese, F. Comparison of Many-Particle Representations for Selected Configuration Interaction: II. Numerical Benchmark Calculations. *J. Chem. Theory Comput.* **2021**, *17*, 2868–2885.
- (24) Chakravorty, S. J.; Gwaltney, S. R.; Davidson, E. R.; Parpia, F. A.; p Fischer, C. F. Ground-State Correlation Energies for Atomic Ions with 3 to 18 Electrons. *Phys. Rev. A* **1993**, *47*, 3649–3670.
- (25) Grimme, S.; Antony, J.; Ehrlich, S.; Krieg, H. A Consistent and Accurate *ab initio* Parametrization of Density Functional Dispersion Correction (DFT-D) for the 94 Elements H-Pu. *J. Chem. Phys.* **2010**, *132*, 154104.
- (26) Yu, L.-J.; Sarrami, F.; O'Reilly, R. J.; Karton, A. Can DFT and *ab initio* Methods Describe All Aspects of the Potential Energy Surface of Cycloreversion Reactions? *Mol. Phys.* **2016**, *114*, 21–33.
- (27) Yu, L.-J.; Sarrami, F.; O'Reilly, R. J.; Karton, A. Reaction Barrier Heights for Cycloreversion of Heterocyclic Rings: An Achilles' Heel for DFT and Standard *ab initio* Procedures. *Chem. Phys.* **2015**, *458*, 1–8.
- (28) Karton, A.; O'Reilly, R. J.; Chan, B.; Radom, L. Determination of Barrier Heights for Proton Exchange in Small Water, Ammonia, and Hydrogen Fluoride Clusters with G4(MP2)-Type, MPn, and SCS-MPn Procedures—A Caveat. *J. Chem. Theory Comput.* **2012**, *8*, 3128–3136.
- (29) Vydrov, O. A.; Van Voorhis, T. Benchmark Assessment of the Accuracy of Several Van Der Waals Density Functionals. *J. Chem. Theory Comput.* **2012**, *8*, 1929–1934.
- (30) Bauza, A.; Alkorta, I.; Frontera, A.; Elguero, J. On the Reliability of Pure and Hybrid DFT Methods for the Evaluation of Halogen, Chalcogen, and Pnicogen Bonds Involving Anionic and Neutral Electron Donors. *J. Chem. Theory Comput.* **2013**, *9*, 5201–5210.

- (31) Bryantsev, V. S.; Diallo, M. S.; van Duin, A. C. T.; Goddard, W. A., III Evaluation of B3LYP, X3LYP, and M06-Class Density Functionals for Predicting the Binding Energies of Neutral, Protonated, and Deprotonated Water Clusters. *J. Chem. Theory Comput.* **2009**, *5*, 1016–1026.
- (32) Schwabe, T. An Isomeric Reaction Benchmark Set to Test If the Performance of State-of-the-Art Density Functionals Can Be Regarded as Independent of the External Potential. *Phys. Chem. Chem. Phys.* **2014**, *16*, 14559–14567.
- (33) Yu, L.-J.; Karton, A. Assessment of Theoretical Procedures for a Diverse Set of Isomerization Reactions Involving Double-bond Migration in Conjugated Dienes. *Chem. Phys.* **2014**, *441*, 166–177.
- (34) Steinmann, S. N.; Csonka, G.; Corminboeuf, C. Unified Inter- and Intramolecular Dispersion Correction Formula for Generalized Gradient Approximation Density Functional Theory. *J. Chem. Theory Comput.* **2009**, *5*, 2950–2958.
- (35) Zhao, Y.; Truhlar, D. G. Benchmark Databases for Nonbonded Interactions and Their Use To Test Density Functional Theory. *J. Chem. Theory Comput.* **2005**, *1*, 415–432.
- (36) Schreiner, P. R.; Fokin, A. A.; Pascal, R. A.; de Meijere, A. Many Density Functional Theory Approaches Fail to Give Reliable Large Hydrocarbon Isomer Energy Differences. *Org. Lett.* **2006**, *8*, 3635–3638.
- (37) Lepetit, C.; Chermette, H.; Gicquel, M.; Heully, J.-L.; Chauvin, R. Description of Carbo-oxocarbons and Assessment of Exchange-Correlation Functionals for the DFT Description of Carbo-mers. *J. Phys. Chem. A* **2007**, *111*, 136–149.
- (38) Johnson, E. R.; Mori-Sanchez, P.; Cohen, A. J.; Yang, W. Delocalization Errors in Density Functionals and Implications for Main-Group Thermochemistry. *J. Chem. Phys.* **2008**, *129*, 204112.

- (39) Zhao, Y.; Truhlar, D. G. Assessment of Density Functionals for π Systems: Energy Differences Between Cumulenes and Poly-ynes; Proton Affinities, Bond Length Alternation, and Torsional Potentials of Conjugated Polyenes; and Proton Affinities of Conjugated Schiff Bases. *J. Phys. Chem. A* **2006**, *110*, 10478–10486.
- (40) Goerigk, L.; Sharma, R. The INV24 Test Set: How Well Do Quantum-chemical Methods Describe Inversion and Racemization Barriers? *Can. J. Chem.* **2016**, *94*, 1133–1143.
- (41) Sure, R.; Hansen, A.; Schwerdtfeger, P.; Grimme, S. Comprehensive Theoretical Study of All 1812 C₆₀ Isomers. *Phys. Chem. Chem. Phys.* **2017**, *19*, 14296–14305.
- (42) Schwabe, T.; Grimme, S. Double-hybrid Density Functionals with Long-range Dispersion Corrections: Higher Accuracy and Extended Applicability. *Phys. Chem. Chem. Phys.* **2007**, *9*, 3397–3406.
- (43) Grimme, S. Seemingly Simple Stereoelectronic Effects in Alkane Isomers and the S-69 Implications for Kohn–Sham Density Functional Theory. *Angew. Chem. Int. Ed.* **2006**, *45*, 4460–4464.
- (44) Csonka, G. I.; French, A. D.; Johnson, G. P.; Stortz, C. A. Evaluation of Density Functionals and Basis Sets for Carbohydrates. *J. Chem. Theory Comput.* **2009**, *5*, 679–692.
- (45) Kruse, H.; Mladek, A.; Gkionis, K.; Hansen, A.; Grimme, S.; Sponer, J. Quantum Chemical Benchmark Study on 46 RNA Backbone Families Using a Dinucleotide Unit. *J. Chem. Theory Comput.* **2015**, *11*, 4972–4991.
- (46) Li, S.; Smith, D. G. A.; Patkowski, K. An Accurate Benchmark Description of the Interactions Between Carbon Dioxide and Polyheterocyclic Aromatic Compounds Containing Nitrogen. *Phys. Chem. Chem. Phys.* **2015**, *17*, 16560–16574.

- (47) Wu, D.; Truhlar, D. G. How Accurate Are Approximate Density Functionals for Noncovalent Interaction of Very Large Molecular Systems? *J. Chem. Theory Comput.* **2021**, *17*, 3967–3973.
- (48) Karton, A.; O'Reilly, R. J.; Radom, L. Assessment of Theoretical Procedures for Calculating Barrier Heights for a Diverse Set of Water-Catalyzed Proton-Transfer Reactions. *J. Phys. Chem. A* **2012**, *116*, 4211–4221.
- (49) Witte, J.; Goldey, M.; Neaton, J. B.; Head-Gordon, M. Beyond Energies: Geometries of Nonbonded Molecular Complexes as Metrics for Assessing Electronic Structure Approaches. *J. Chem. Theory Comput.* **2015**, *11*, 1481–1492.
- (50) Steinmann, S. N.; Piemontesi, C.; Delacht, A.; Corminboeuf, C. Why Are the Interaction Energies of Charge-Transfer Complexes Challenging for DFT? *J. Chem. Theory Comput.* **2012**, *8*, 1629–1640.
- (51) Lao, K. U.; Herbert, J. M. Accurate and Efficient Quantum Chemistry Calculations for Noncovalent Interactions in Many-Body Systems: The XSAPT Family of Methods. *J. Phys. Chem. A* **2015**, *119*, 235–252.
- (52) Mardirossian, N.; Lambrecht, D. S.; McCaslin, L.; Xantheas, S. S.; Head-Gordon, M. The Performance of Density Functionals for Sulfate–Water Clusters. *J. Chem. Theory Comput.* **2013**, *9*, 1368–1380.
- (53) Granatier, J.; Pitonak, M.; Hobza, P. Accuracy of Several Wave Function and Density Functional Theory Methods for Description of Noncovalent Interaction of Saturated and Unsaturated Hydrocarbon Dimers. *J. Chem. Theory Comput.* **2012**, *8*, 2282–2292.
- (54) Lao, K. U.; Schaeffer, R.; Jansen, G.; Herbert, J. M. Accurate Description of Intermolecular Interactions Involving Ions Using Symmetry-Adapted Perturbation Theory. *J. Chem. Theory Comput.* **2015**, *11*, 2473–2486.

- (55) Karton, A.; Gruzman, D.; Martin, J. M. L. Benchmark Thermochemistry of the C_nH_{2n+2} Alkane Isomers ($n = 2-8$) and Performance of DFT and Composite *ab initio* Methods for Dispersion-Driven Isomeric Equilibria. *J. Phys. Chem. A* **2009**, *113*, 8434–8447.
- (56) Kozuch, S.; Bachrach, S. M.; Martin, J. M. L. Conformational Equilibria in Butane-1,4-diol: A Benchmark of a Prototypical System with Strong Intramolecular H-bonds. *J. Phys. Chem. A* **2014**, *118*, 293–303.
- (57) Yu, L.-J.; Sarrami, F.; Karton, A.; O'Reilly, R. J. An Assessment of Theoretical Procedures for π -conjugation Stabilisation Energies in Enones. *Mol. Phys.* **2015**, *113*, 1284–1296.
- (58) Gruzman, D.; Karton, A.; Martin, J. M. L. Performance of *ab initio* and Density Functional Methods for Conformational Equilibria of C_nH_{2n+2} Alkane Isomers ($n = 4-8$). *J. Phys. Chem. A* **2009**, *113*, 11974–11983.
- (59) Wilke, J. J.; Lind, M. C.; Schaefer, H. F., III; Csaszar, A. G.; Allen, W. D. Conformers of Gaseous Cysteine. *J. Chem. Theory Comput.* **2009**, *5*, 1511–1523.
- (60) Martin, J. M. L. What Can We Learn About Dispersion From the Conformer Surface of N-Pentane? *J. Phys. Chem. A* **2013**, *117*, 3118–3132.
- (61) Grimme, S.; Kruse, H.; Goerigk, L.; Erker, G. The Mechanism of Dihydrogen Activation by Frustrated Lewis Pairs Revisited. *Angew. Chem. Int. Ed.* **2010**, *49*, 1402–1405.
- (62) Sherrill, C. D.; Takatani, T.; Hohenstein, E. G. An Assessment of Theoretical Methods for Nonbonded Interactions: Comparison to Complete Basis Set Limit Coupled-Cluster Potential Energy Curves for the Benzene Dimer, the Methane Dimer, Benzene–Methane, and Benzene– H_2S . *J. Phys. Chem. A* **2009**, *113*, 10146–10159.

- (63) Leverentz, H. R.; Siepmann, J. I.; Truhlar, D. G.; Loukonen, V.; Vehkamäki, H. Energetics of Atmospherically Implicated Clusters Made of Sulfuric Acid, Ammonia, and Dimethyl Amine. *J. Phys. Chem. A* **2013**, *117*, 3819–3825.
- (64) Grimme, S.; Mück-Lichtenfeld, C.; Würthwein, E.-U.; Ehlert, A. W.; Goumans, T.; Lammertsma, K. Consistent Theoretical Description of 1,3-Dipolar Cycloaddition Reactions. *J. Phys. Chem. A* **2006**, *110*, 2583–2586.
- (65) Piacenza, M.; Grimme, S. Systematic Quantum Chemical Study of DNA-Base Tautomers. *J. Comput. Chem.* **2004**, *25*, 83–99.
- (66) Woodcock, H. L.; Schaefer, H. F.; Schreiner, P. R. Problematic Energy Differences Between Cumulenes and Poly-ynes: Does This Point to a Systematic Improvement of Density Functional Theory? *J. Phys. Chem. A* **2002**, *106*, 11923–11931.
- (67) Karton, A.; Martin, J. M. L. Explicitly Correlated Benchmark Calculations on C₈H₈ Isomer Energy Separations: How Accurate are DFT, Double-Hybrid, and Composite *ab initio* Procedures? *Mol. Phys.* **2012**, *110*, 2477–2491.
- (68) Zhao, Y.; Tishchenko, O.; Gour, J. R.; Li, W.; Lutz, J. J.; Piecuch, P.; Truhlar, D. G. Thermochemical Kinetics for Multireference Systems: Addition Reactions of Ozone. *J. Phys. Chem. A* **2009**, *113*, 5786–5799.
- (69) Manna, D.; Martin, J. M. L. What Are the Ground State Structures of C₂₀ and C₂₄? An Explicitly Correlated *ab initio* Approach. *J. Phys. Chem. A* **2016**, *120*, 153–160.
- (70) Ess, D. H.; Houk, K. Activation Energies of Pericyclic Reactions: Performance of DFT, MP2, and CBS-QB3 Methods for the Prediction of Activation Barriers and Reaction Energetics of 1,3-Dipolar Cycloadditions, and Revised Activation Enthalpies for a Standard Set of Hydrocarbon Pericyclic Reactions. *J. Phys. Chem. A* **2005**, *109*, 9542–9553.

- (71) Dinadayalane, T.; Vijaya, R.; Smitha, A.; Sastry, G. Diels–Alder Reactivity of Butadiene and Cyclic Five-Membered Dienes ((CH)₄X, X = CH₂, SiH₂, O, NH, PH, and S) with Ethylene: A Benchmark Study. *J. Phys. Chem. A* **2002**, *106*, 1627–1633.
- (72) Setiawan, D.; Kraka, E.; Cremer, D. Strength of the Pnicogen Bond in Complexes Involving Group Va Elements N, P, and As. *J. Phys. Chem. A* **2015**, *119*, 1642–1656.
- (73) Kozuch, S.; Martin, J. M. L. Halogen Bonds: Benchmarks and Theoretical Analysis. *J. Chem. Theory Comput.* **2013**, *9*, 1918–1931.
- (74) Rezac, J.; Riley, K. E.; Hobza, P. Benchmark Calculations of Noncovalent Interactions of Halogenated Molecules. *J. Chem. Theory Comput.* **2012**, *8*, 4285–4292.
- (75) Grimme, S.; Steinmetz, M.; Korth, M. How to Compute Isomerization Energies of Organic Molecules with Quantum Chemical Methods. *J. Org. Chem.* **2007**, *72*, 2118–2126.
- (76) Řeha, D.; Valdes, H.; Vondrášek, J.; Hobza, P.; Abu-Riziq, A.; Crews, B.; De Vries, M. S. Structure and IR Spectrum of Phenylalanyl–Glycyl–Glycine Tripeptide in the Gas-Phase: IR/UV Experiments, *ab initio* Quantum Chemical Calculations, and Molecular Dynamic Simulations. *Chem. Eur. J.* **2005**, *11*, 6803–6817.
- (77) Goerigk, L.; Karton, A.; Martin, J. M. L.; Radom, L. Accurate Quantum Chemical Energies for Tetrapeptide Conformations: Why MP2 Data with an Insufficient Basis Set Should Be Handled with Caution. *Phys. Chem. Chem. Phys.* **2013**, *15*, 7028–7031.
- (78) Fogueri, U. R.; Kozuch, S.; Karton, A.; Martin, J. M. L. The Melatonin Conformer Space: Benchmark and Assessment of Wave Function and DFT Methods for a Paradigmatic Biological and Pharmacological Molecule. *J. Phys. Chem. A* **2013**, *117*, 2269–2277.

- (79) Kesharwani, M. K.; Karton, A.; Martin, J. M. L. Benchmark *ab initio* Conformational Energies for the Proteinogenic Amino Acids Through Explicitly Correlated Methods. Assessment of Density Functional Methods. *J. Chem. Theory Comput.* **2016**, *12*, 444–454.
- (80) Rezac, J.; Huang, Y.; Hobza, P.; Beran, G. J. O. Benchmark Calculations of Three-Body Intermolecular Interactions and the Performance of Low-Cost Electronic Structure Methods. *J. Chem. Theory Comput.* **2015**, *11*, 3065–3079.
- (81) Faver, J. C.; Benson, M. L.; He, X.; Roberts, B. P.; Wang, B.; Marshall, M. S.; Kennedy, M. R.; Sherrill, C. D.; Merz, K. M., Jr. Formal Estimation of Errors in Computed Absolute Interaction Energies of Protein–Ligand Complexes. *J. Chem. Theory Comput.* **2011**, *7*, 790–797.
- (82) Ni, Z.; Guo, Y.; Neese, F.; Li, W.; Li, S. Cluster-in-molecule Local Correlation Method with an Accurate Distant Pair Correction for Large Systems. *J. Chem. Theory Comput.* **2021**, *17*, 756–766.
- (83) de Lange, K. M.; Lane, J. R. Explicit correlation and intermolecular interactions: Investigating carbon dioxide complexes with the CCSD(T)-F12 method. *J. Chem. Phys.* **2011**, *134*, 034301.
- (84) McMahon, J. D.; Lane, J. R. Explicit Correlation and Basis Set Superposition Error: The Structure and Energy of Carbon Dioxide Dimer. *J. Chem. Phys.* **2011**, *135*, 154309.
- (85) Rezac, J.; Hobza, P. Describing Noncovalent Interactions Beyond the Common Approximations: How Accurate is the “Gold Standard”, CCSD(T) at the Complete Basis Set Limit? *J. Chem. Theory Comput.* **2013**, *9*, 2151–2155.
- (86) Crittenden, D. L. A Systematic CCSD(T) Study of Long-Range and Noncovalent Interactions Between Benzene and a Series of First- and Second-Row Hydrides and Rare Gas Atoms. *J. Phys. Chem. A* **2009**, *113*, 1663–1669.

- (87) Mintz, B. J.; Parks, J. M. Benchmark Interaction Energies for Biologically Relevant Noncovalent Complexes Containing Divalent Sulfur. *J. Phys. Chem. A* **2012**, *116*, 1086–1092.
- (88) Copeland, K. L.; Tschumper, G. S. Hydrocarbon/Water Interactions: Encouraging Energetics and Structures From DFT but Disconcerting Discrepancies for Hessian Indices. *J. Chem. Theory Comput.* **2012**, *8*, 1646–1656.
- (89) Temelso, B.; Archer, K. A.; Shields, G. C. Benchmark Structures and Binding Energies of Small Water Clusters with Anharmonicity Corrections. *J. Phys. Chem. A* **2011**, *115*, 12034–12046.
- (90) Boese, A. D. Basis Set Limit Coupled-Cluster Studies of Hydrogen-bonded Systems. *Mol. Phys.* **2015**, *113*, 1618–1629.
- (91) Fanourgakis, G. S.; Apra, E.; Xantheas, S. S. High-level *ab initio* Calculations for the Four Low-lying Families of Minima of $(\text{H}_2\text{O})_{20}$. I. Estimates of MP2/CBS Binding Energies and Comparison with Empirical Potentials. *J. Chem. Phys.* **2004**, *121*, 2655–2663.
- (92) Smith, D. G. A.; Jankowski, P.; Slawik, M.; Witek, H. A.; Patkowski, K. Basis Set Convergence of the Post-CCSD(T) Contribution to Noncovalent Interaction Energies. *J. Chem. Theory Comput.* **2014**, *10*, 3140–3150.
- (93) Yoo, S.; Apra, E.; Zeng, X. C.; Xantheas, S. S. High-level *ab initio* Electronic Structure Calculations of Water Clusters $(\text{H}_2\text{O})_{16}$ and $(\text{H}_2\text{O})_{17}$: A New Global Minimum for $(\text{H}_2\text{O})_{16}$. *J. Phys. Chem. Lett.* **2010**, *1*, 3122–3127.
- (94) Hohenstein, E. G.; Sherrill, C. D. Effects of Heteroatoms on Aromatic π - π Interactions: Benzene-Pyridine and Pyridine Dimer. *J. Phys. Chem. A* **2009**, *113*, 878–886.

- (95) Takatani, T.; Sherrill, C. D. Performance of Spin-component-scaled Møller–Plesset Theory (SCS-MP2) for Potential Energy Curves of Noncovalent Interactions. *Phys. Chem. Chem. Phys.* **2007**, *9*, 6106–6114.
- (96) Jurecka, P.; Sponer, J.; Cerny, J.; Hobza, P. Benchmark Database of Accurate (MP2 and CCSD(T) Complete Basis Set Limit) Interaction Energies of Small Model Complexes, DNA Base Pairs, and Amino Acid Pairs. *Phys. Chem. Chem. Phys.* **2006**, *8*, 1985–1993.
- (97) Lee, J. S. Accurate *ab initio* Binding Energies of Alkaline Earth Metal Clusters. *J. Phys. Chem. A* **2005**, *109*, 11927–11932.
- (98) Friedrich, J.; Haenchen, J. Incremental CCSD(T)(F12*)|MP2: A Black Box Method To Obtain Highly Accurate Reaction Energies. *J. Chem. Theory Comput.* **2013**, *9*, 5381–5394.
- (99) Rezac, J.; Riley, K. E.; Hobza, P. S66: A Well-balanced Database of Benchmark Interaction Energies Relevant to Biomolecular Structures. *J. Chem. Theory Comput.* **2011**, *7*, 2427–2438.
- (100) Li, X.; Xu, X.; You, X.; Truhlar, D. G. Benchmark Calculations for Bond Dissociation Enthalpies of Unsaturated Methyl Esters and the Bond Dissociation Enthalpies of Methyl Linolenate. *J. Phys. Chem. A* **2016**, *120*, 4025–4036.
- (101) Guner, V.; Khuong, K.; Leach, A.; Lee, P.; Bartberger, M.; Houk, K. A Standard Set of Pericyclic Reactions of Hydrocarbons for the Benchmarking of Computational Methods: The Performance of *ab initio*, Density Functional, CASSCF, CASPT2, and CBS-QB3 Methods for the Prediction of Activation Barriers, Reaction Energetics, and Transition State Geometries. *J. Phys. Chem. A* **2003**, *107*, 11445–11459.
- (102) Tentscher, P. R.; Arey, J. S. Binding in Radical-Solvent Binary Complexes: Bench-

- mark Energies and Performance of Approximate Methods. *J. Chem. Theory Comput.* **2013**, *9*, 1568–1579.
- (103) Jiang, W.; Laury, M. L.; Powell, M.; Wilson, A. K. Comparative Study of Single and Double Hybrid Density Functionals for the Prediction of 3d Transition Metal Thermochemistry. *J. Chem. Theory Comput.* **2012**, *8*, 4102–4111.
- (104) Zhang, W.; Truhlar, D. G.; Tang, M. Tests of Exchange-Correlation Functional Approximations Against Reliable Experimental Data for Average Bond Energies of 3d Transition Metal Compounds. *J. Chem. Theory Comput.* **2013**, *9*, 3965–3977.
- (105) Posada-Borbón, A.; Posada-Amarillas, A. Theoretical Study of Homonuclear and Binary Transition-Metal Dimers. *Chem. Phys. Lett.* **2015**, *618*, 66–71.
- (106) Chan, B.; Gill, P. M.; Kimura, M. Assessment of DFT Methods for Transition Metals with the TMC151 Compilation of Data Sets and Comparison with Accuracies for Main-Group Chemistry. *J. Chem. Theory Comput.* **2019**, *15*, 3610–3622.
- (107) Chan, B. The CUAGAU Set of Coupled-cluster Reference Data for Small Copper, Silver, and Gold Compounds and Assessment of DFT Methods. *J. Phys. Chem. A* **2019**, *123*, 5781–5788.
- (108) Chan, B. Assessment and Development of DFT with the Expanded CUAGAU-2 Set of Group-11 Cluster Systems. *Int. J. Quantum Chem.* **2021**, *121*, e26453.
- (109) Aebersold, L. E.; Yuwono, S. H.; Schoendorff, G.; Wilson, A. K. Efficacy of Density Functionals and Relativistic Effective Core Potentials for Lanthanide-containing Species: The Ln54 Molecule Set. *J. Chem. Theory Comput.* **2017**, *13*, 2831–2839.
- (110) Aebersold, L. E.; Wilson, A. K. Considering Density Functional Approaches for Actinide Species: The An66 Molecule Set. *J. Phys. Chem. A* **2021**, *125*, 7029–7037.

- (111) Jiang, W.; DeYonker, N. J.; Determan, J. J.; Wilson, A. K. Toward Accurate Theoretical Thermochemistry of First-Row Transition Metal Complexes. *The Journal of Physical Chemistry A* **2012**, *116*, 870–885.
- (112) Averkiev, B. B.; Zhao, Y.; Truhlar, D. G. Binding Energy of D10 Transition Metals to Alkenes by Wave Function Theory and Density Functional Theory. *J. Mol. Catal. A Chem.* **2010**, *324*, 80–88.
- (113) Xu, X.; Zhang, W.; Tang, M.; Truhlar, D. G. Do Practical Standard Coupled Cluster Calculations Agree Better Than Kohn–Sham Calculations with Currently Available Functionals When Compared to the Best Available Experimental Data for Dissociation Energies of Bonds to 3d Transition Metals? *J. Chem. Theory Comput.* **2015**, *11*, 2036–2052.
- (114) DeYonker, N. J.; Peterson, K. A.; Steyl, G.; Wilson, A. K.; Cundari, T. R. Quantitative Computational Thermochemistry of Transition Metal Species. *J. Phys. Chem. A* **2007**, *111*, 11269–11277.
- (115) Stein, C. J.; von Burg, V.; Reiher, M. The Delicate Balance of Static and Dynamic Electron Correlation. *J. Chem. Theory Comput.* **2016**, *12*, 3764–3773.
- (116) North, S. C.; Wilson, A. K. *ab initio* Composite Approaches for Heavy Element Energetics: Ionization Potentials for the Actinide Series of Elements. *J. Phys. Chem. A* **2022**, *126*, 3027–3042.
- (117) S Almeida, N. M.; Melin, T. R.; North, S. C.; Welch, B. K.; Wilson, A. K. *ab initio* Composite Strategies and Multireference Approaches for Lanthanide Sulfides and Selenides. *J. Chem. Phys.* **2022**, *157*.
- (118) Peterson, C.; Penchoff, D. A.; Wilson, A. K. *ab initio* Approaches for the Determination of Heavy Element Energetics: Ionization Energies of Trivalent Lanthanides (Ln = La–Eu). *J. Chem. Phys.* **2015**, *143*.

- (119) Weymuth, T.; Couzijn, E. P. A.; Chen, P.; Reiher, M. New Benchmark Set of Transition-Metal Coordination Reactions for the Assessment of Density Functionals. *J. Chem. Theory Comput.* **2014**, *10*, 3092–3103.
- (120) Sun, Y.; Chen, H. Performance of Density Functionals for Activation Energies of Zr-Mediated Reactions. *J. Chem. Theory Comput.* **2013**, *9*, 4735–4743.
- (121) Sun, Y.; Chen, H. Performance of Density Functionals for Activation Energies of Re-Catalyzed Organic Reactions. *J. Chem. Theory Comput.* **2014**, *10*, 579–588.
- (122) Hu, L.; Chen, H. Assessment of DFT Methods for Computing Activation Energies of Mo/W-Mediated Reactions. *J. Chem. Theory Comput.* **2015**, *11*, 4601–4614.
- (123) Maurer, L. R.; Bursch, M.; Grimme, S.; Hansen, A. Assessing Density Functional Theory for Chemically Relevant Open-Shell Transition Metal Reactions. *J. Chem. Theory Comput.* **2021**, *17*, 6134–6151.
- (124) Marshall, M. S.; Burns, L. A.; Sherrill, C. D. Basis Set Convergence of the Coupled-cluster Correction, $\delta_{MP2}^{CCSD(T)}$: Best Practices for Benchmarking Non-covalent Interactions and the Attendant Revision of the S22, NBC10, HBC6, and HSG Databases. *J. Chem. Phys.* **2011**, *135*, 194102.
- (125) Lao, K. U.; Herbert, J. M. An Improved Treatment of Empirical Dispersion and a Many-body Energy Decomposition Scheme for the Explicit Polarization Plus Symmetry-adapted Perturbation Theory (xsapt) Method. *J. Chem. Phys.* **2013**, *139*, 034107.
- (126) Neese, F.; Schwabe, T.; Kossmann, S.; Schirmer, B.; Grimme, S. Assessment of Orbital-Optimized, Spin-Component Scaled Second-Order Many-Body Perturbation Theory for Thermochemistry and Kinetics. *J. Chem. Theory Comput.* **2009**, *5*, 3060–3073.

- (127) Parthiban, S.; Martin, J. M. Assessment of W1 and W2 Theories for the Computation of Electron Affinities, Ionization Potentials, Heats of Formation, and Proton Affinities. *J. Chem. Phys.* **2001**, *114*, 6014–6029.
- (128) Chan, B.; Gilbert, A. T.; Gill, P. M.; Radom, L. Performance of Density Functional Theory Procedures for the Calculation of Proton-Exchange Barriers: Unusual Behavior of M06-Type Functionals. *J. Chem. Theory Comput.* **2014**, *10*, 3777–3783.
- (129) Zhao, Y.; Lynch, B. J.; Truhlar, D. G. Multi-coefficient Extrapolated Density Functional Theory for Thermochemistry and Thermochemical Kinetics. *Phys. Chem. Chem. Phys.* **2005**, *7*, 43–52.
- (130) Otero-De-La-Roza, A.; Johnson, E. R.; DiLabio, G. A. Halogen Bonding From Dispersion-Corrected Density-Functional Theory: The Role of Delocalization Error. *J. Chem. Theory Comput.* **2014**, *10*, 5436–5447.
- (131) Rezac, J.; Hobza, P. Advanced Corrections of Hydrogen Bonding and Dispersion for Semiempirical Quantum Mechanical Methods. *J. Chem. Theory Comput.* **2012**, *8*, 141–151.
- (132) Boese, A. D. Density Functional Theory and Hydrogen Bonds: Are We There Yet? *ChemPhysChem* **2015**, *16*, 978–985.
- (133) Anacker, T.; Friedrich, J. New Accurate Benchmark Energies for Large Water Clusters: DFT Is Better Than Expected. *J. Comput. Chem.* **2014**, *35*, 634–643.
- (134) Curtiss, L.; Raghavachari, K.; Redfern, P.; Pople, J. Assessment of Gaussian-2 and Density Functional Theories for the Computation of Enthalpies of Formation. *J. Chem. Phys.* **1997**, *106*, 1063–1079.
- (135) Krieg, H.; Grimme, S. Thermochemical Benchmarking of Hydrocarbon Bond Sep-

- aration Reaction Energies: Jacob's Ladder is not Reversed! *Mol. Phys.* **2010**, *108*, 2655–2666.
- (136) Zheng, J.; Zhao, Y.; Truhlar, D. G. Representative Benchmark Suites for Barrier Heights of Diverse Reaction Types and Assessment of Electronic Structure Methods for Thermochemical Kinetics. *J. Chem. Theory Comput.* **2007**, *3*, 569–582.
- (137) Karton, A.; Tarnopolsky, A.; Lamere, J.-F.; Schatz, G. C.; Martin, J. M. L. Highly Accurate First-Principles Benchmark Data Sets for the Parametrization and Validation of Density Functional and Other Approximate Methods. Derivation of a Robust, Generally Applicable, Double-Hybrid Functional for Thermochemistry and Thermochemical Kinetics. *J. Phys. Chem. A* **2008**, *112*, 12868–12886.
- (138) Friedrich, J. Efficient Calculation of Accurate Reaction Energies—Assessment of Different Models in Electronic Structure Theory. *J. Chem. Theory Comput.* **2015**, *11*, 3596–3609.
- (139) Lynch, B. J.; Zhao, Y.; Truhlar, D. G. Effectiveness of Diffuse Basis Functions for Calculating Relative Energies by Density Functional Theory. *J. Phys. Chem. A* **2003**, *107*, 1384–1388.
- (140) Fracchia, F.; Cimiraglia, R.; Angeli, C. Assessment of multireference perturbation methods for chemical reaction barrier heights. *J. Phys. Chem. A* **2015**, *119*, 5490–5495.
- (141) Husch, T.; Freitag, L.; Reiher, M. Calculation of Ligand Dissociation Energies in Large Transition-Metal Complexes. *J. Chem. Theory Comput.* **2018**, *14*, 2456–2468.
- (142) Yao, Y.; Giner, E.; Li, J.; Toulouse, J.; Umrigar, C. Almost Exact Energies for the Gaussian-2 Set with the Semistochastic Heat-Bath Configuration Interaction Method. *The Journal of Chemical Physics* **2020**, *153*.

- (143) Send, R.; Kühn, M.; Furche, F. Assessing Excited State Methods by Adiabatic Excitation Energies. *J. Chem. Theory Comput.* **2011**, *7*, 2376–2386.
- (144) Yang, K.; Peverati, R.; Truhlar, D. G.; Valero, R. Density Functional Study of Multiplicity- Changing Valence and Rydberg Excitations of P-block Elements: Delta Self-consistent Field, Collinear Spin-flip Time-dependent Density Functional Theory (DFT), and Conventional Time- Dependent DFT. *J. Chem. Phys.* **2011**, *135*, 044118.
- (145) Loos, P.-F.; Scemama, A.; Boggio-Pasqua, M.; Jacquemin, D. Mountaineering Strategy to Excited States: Highly Accurate Energies and Benchmarks for Exotic Molecules and Radicals. *J. Chem. Theory Comput.* **2020**, *16*, 3720–3736.
- (146) Hoyer, C. E.; Gagliardi, L.; Truhlar, D. G. Multiconfiguration Pair-Density Functional Theory Spectral Calculations Are Stable to Adding Diffuse Basis Functions. *J. Phys. Chem. Lett.* **2015**, *6*, 4184–4188.
- (147) Song, Y.; Guo, Y.; Lei, Y.; Zhang, N.; Liu, W. The Static-Dynamic-Static Family of Methods for Strongly Correlated Electrons: Methodology and Benchmarking. *Top. Curr. Chem.* **2021**, *379*, 43.
- (148) Stein, T.; Kronik, L.; Baer, R. Reliable Prediction of Charge Transfer Excitations in Molecular Complexes Using Time-Dependent Density Functional Theory. *J. Am. Chem. Soc.* **2009**, *131*, 2818–2820.
- (149) Isegawa, M.; Truhlar, D. G. Valence Excitation Energies of Alkenes, Carbonyl Compounds, and Azabenzenes by Time-dependent Density Functional Theory: Linear Response of the Ground State Compared to Collinear and Noncollinear Spin-flip TDDFT with the Tamm- Dancoff Approximation. *J. Chem. Phys.* **2013**, *138*, 134111.
- (150) Jacquemin, D.; Perpète, E. A.; Vydrov, O. A.; Scuseria, G. E.; Adamo, C. Assess-

- ment of Long-range Corrected Functionals Performance for $n \rightarrow \pi^*$ Transitions in Organic Dyes. *J. Chem. Phys.* **2007**, *127*.
- (151) Jacquemin, D.; Perpète, E. A.; Scuseria, G. E.; Ciofini, I.; Adamo, C. Td-dft Performance for the Visible Absorption Spectra of Organic Dyes: Conventional Versus Long-range Hybrids. *J. Chem. Theory Comput.* **2008**, *4*, 123–135.
- (152) Jacquemin, D.; Wathélet, V.; Perpète, E. A.; Adamo, C. Extensive TD-DFT Benchmark: Singlet-Excited States of Organic Molecules. *J. Chem. Theory Comput.* **2009**, *5*, 2420–2435.
- (153) Jacquemin, D.; Planchat, A.; Adamo, C.; Mennucci, B. TD-DFT Assessment of Functionals for Optical 0–0 Transitions in Solvated Dyes. *J. Chem. Theory Comput.* **2012**, *8*, 2359–2372.
- (154) Parac, M.; Grimme, S. Comparison of Multireference Møller-Plesset Theory and Time-dependent Methods for the Calculation of Vertical Excitation Energies of Molecules. *J. Phys. Chem. A* **2002**, *106*, 6844–6850.
- (155) Goerigk, L.; Moellmann, J.; Grimme, S. Computation of Accurate Excitation Energies for Large Organic Molecules with Double-hybrid Density Functionals. *Phys. Chem. Chem. Phys.* **2009**, *11*, 4611–4620.
- (156) Dierksen, M.; Grimme, S. Density Functional Calculations of the Vibronic Structure of Electronic Absorption Spectra. *J. Chem. Phys.* **2004**, *120*, 3544–3554.
- (157) Van Faassen, M.; de Boeij, P. Excitation Energies for a Benchmark Set of Molecules Obtained Within Time-Dependent Current-Density Functional Theory Using the Vignale–Kohn Functional. *J. Chem. Phys.* **2004**, *120*, 8353–8363.
- (158) Fabian, J. Electronic Excitation of Sulfur-Organic Compounds—Performance of Time-Dependent Density Functional Theory. *Theor. Chem. Acc.* **2001**, *106*, 199–217.

- (159) Matsuura, A.; Sato, H.; Sotoyama, W.; Takahashi, A.; Sakurai, M. Am1, PM3, and PM5 Calculations of the Absorption Maxima of Basic Organic Dyes. *J. Mol. Struct: THEOCHEM* **2008**, *860*, 119–127.
- (160) Rohrdanz, M. A.; Herbert, J. M. Simultaneous Benchmarking of Ground-and Excited-State Properties with Long-Range-Corrected Density Functional Theory. *J. Chem. Phys.* **2008**, *129*.
- (161) Fransson, T.; Brumboiu, I. E.; Vidal, M. L.; Norman, P.; Coriani, S.; Dreuw, A. Xa-boom: An X-ray Absorption Benchmark of Organic Molecules Based on Carbon, Nitrogen, and Oxygen $1s \rightarrow \pi^*$ Transitions. *J. Chem. Theory Comput.* **2021**, *17*, 1618–1637.
- (162) Guido, C. A.; Knecht, S.; Kongsted, J.; Mennucci, B. Benchmarking Time-dependent Density Functional Theory for Excited State Geometries of Organic Molecules in Gas-phase and in Solution. *J. Chem. Theory Comput.* **2013**, *9*, 2209–2220.
- (163) Shao, Y.; Mei, Y.; Sundholm, D.; Kaila, V. R. Benchmarking the Performance of Time-dependent Density Functional Theory Methods on Biochromophores. *J. Chem. Theory Comput.* **2019**, *16*, 587–600.
- (164) Grabarz, A. M.; Ośmiałowski, B. Benchmarking Density Functional Approximations for Excited-State Properties of Fluorescent Dyes. *Molecules* **2021**, *26*, 7434.
- (165) Bogo, N.; Stein, C. J. Benchmarking DFT-based Excited-state Methods for Intermolecular Charge-transfer Excitations. *arXiv preprint arXiv:2405.01382* **2024**,
- (166) Loos, P.-F.; Galland, N.; Jacquemin, D. Theoretical 0–0 Energies with Chemical Accuracy. *J. Phys. Chem. Lett.* **2018**, *9*, 4646–4651.
- (167) Alkhatib, Q.; Helal, W.; Marashdeh, A. Accurate Predictions of the Electronic Excited States of BODIPY Based Dye Sensitizers Using Spin-Component-Scaled

- Double-Hybrid Functionals: a TD-DFT Benchmark Study. *RSC Adv.* **2022**, *12*, 1704–1717.
- (168) Isegawa, M.; Peverati, R.; Truhlar, D. G. Performance of Recent and High-performance Approximate Density Functionals for Time-Dependent Density Functional Theory Calculations of Valence and Rydberg Electronic Transition Energies. *J. Chem. Phys.* **2009**, *137*, 224–228.
- (169) Zaari, R. R.; Wong, S. Y. Photoexcitation of 11-z-cis-7, 8-dihydro Retinal and 11-z-cis Retinal: A Comparative Computational Study. *Chem. Phys. Lett.* **2009**, *469*, 224–228.
- (170) Jacquemin, D.; Duchemin, I.; Blase, X. 0–0 Energies Using Hybrid Schemes: Benchmarks of TD-DFT, CIS (d), ADC (2), CC2, and BSE/GW Formalisms for 80 Real-life Compounds. *J. Chem. Theory Comput.* **2015**, *11*, 5340–5359.
- (171) Winter, N. O.; Graf, N. K.; Leutwyler, S.; Hättig, C. Benchmarks for 0–0 Transitions of Aromatic Organic Molecules: DFT/B3LYP, ADC (2), CC2, SOS-CC2 and SCS-CC2 Compared to High-resolution Gas-phase Data. *Phys. Chem. Chem. Phys.* **2013**, *15*, 6623–6630.
- (172) Goerigk, L.; Grimme, S. Assessment of TD-DFT Methods and of Various Spin Scaled CIS (d) and CC2 Versions for the Treatment of Low-lying Valence Excitations of Large Organic Dyes. *J. Chem. Phys.* **2010**, *132*, 184103.
- (173) Filatov, M. Assessment of Density Functional Methods for Obtaining Geometries at Conical Intersections in Organic Molecules. *J. Chem. Theory Comput.* **2013**, *9*, 4526–4541.
- (174) Gronowski, M. Td-dft Benchmark: Excited States of Atoms and Atomic Ions. *Comput. Theor. Chem.* **2017**, *1108*, 50–56.

- (175) Mewes, S. A.; Plasser, F.; Krylov, A.; Dreuw, A. Benchmarking Excited-state Calculations Using Exciton Properties. *J. Chem. Theory Comput.* **2018**, *14*, 710–725.
- (176) Fang, C.; Oruganti, B.; Durbeej, B. How Method-dependent Are Calculated Differences Between Vertical, Adiabatic, and 0–0 Excitation Energies? *J. Phys. Chem. A* **2014**, *118*, 4157–4171.
- (177) Falden, H. H.; Falster-Hansen, K. R.; Bak, K. L.; Rettrup, S.; Sauer, S. P. Benchmarking Second Order Methods for the Calculation of Vertical Electronic Excitation Energies: Valence and Rydberg States in Polycyclic Aromatic Hydrocarbons. *J. Phys. Chem. A* **2009**, *113*, 11995–12012.
- (178) Kozma, B.; Tajti, A.; Demoulin, B.; Izsák, R.; Nooijen, M.; Szalay, P. G. A New Benchmark Set for Excitation Energy of Charge Transfer States: Systematic Investigation of Coupled Cluster Type Methods. *J. Chem. Theory Comput.* **2020**, *16*, 4213–4225.
- (179) Loos, P.-F.; Jacquemin, D. Chemically Accurate 0–0 Energies with Not-so-accurate Excited State Geometries. *J. Chem. Theory Comput.* **2019**, *15*, 2481–2491.
- (180) Loos, P.-F.; Scemama, A.; Blondel, A.; Garniron, Y.; Caffarel, M.; Jacquemin, D. A Mountaineering Strategy to Excited States: Highly Accurate Reference Energies and Benchmarks. *J. Chem. Theory Comput.* **2018**, *14*, 4360–4379.
- (181) Loos, P.-F.; Lipparini, F.; Boggio-Pasqua, M.; Scemama, A.; Jacquemin, D. A Mountaineering Strategy to Excited States: Highly Accurate Energies and Benchmarks for Medium Sized Molecules. *J. Chem. Theory Comput.* **2020**, *16*, 1711–1741.
- (182) Veril, M.; Scemama, A.; Caffarel, M.; Lipparini, F.; Boggio-Pasqua, M.; Jacquemin, D.; Loos, P.-F. Questdb: A Database of Highly Accurate Excitation Energies for the Electronic Structure Community. *WIREs Comput. Mol. Sci.* **2021**, *11*, e1517.

- (183) Loos, P.-F.; Comin, M.; Blase, X.; Jacquemin, D. Reference Energies for Intramolecular Charge-Transfer Excitations. *J. Chem. Theory Comput.* **2021**, *17*, 3666–3686.
- (184) Loos, P.-F.; Jacquemin, D. A Mountaineering Strategy to Excited States: Highly Accurate Energies and Benchmarks for Bicyclic Systems. *J. Phys. Chem. A* **2021**, *125*, 10174–10188.
- (185) Ghosh, S.; Sonnenberger, A. L.; Hoyer, C. E.; Truhlar, D. G.; Gagliardi, L. Multi-configuration Pair-Density Functional Theory Outperforms Kohn–Sham Density Functional Theory and Multireference Perturbation Theory for Ground-State and Excited-State Charge Transfer. *J. Chem. Theory Comput.* **2015**, *11*, 3643–3649.
- (186) Peach, M. J.; Benfield, P.; Helgaker, T.; Tozer, D. J. Excitation Energies in Density Functional Theory: An Evaluation and a Diagnostic Test. *J. Chem. Phys.* **2008**, *128*, 044118.
- (187) Marian, C. M.; Gilka, N. Performance of the Density Functional Theory/multireference Configuration Interaction Method on Electronic Excitation of Extended π -systems. *J. Chem. Theory Comput.* **2008**, *4*, 1501–1515.
- (188) Momeni, M. R.; Brown, A. Why Do TD-DFT Excitation Energies of BODIPY/Aza-BODIPY Families Largely Deviate From Experiment? Answers From Electron Correlated and Multireference Methods. *J. Chem. Theory Comput.* **2015**, *11*, 2619–2632.
- (189) Yang, Y.; Davidson, E. R.; Yang, W. Nature of Ground and Electronic Excited States of Higher Acenes. *PNAS* **2016**, *113*, E5098–E5107.
- (190) Budzák, S.; Scalmani, G.; Jacquemin, D. Accurate Excited-state Geometries: A CASPT2 and Coupled-Cluster Reference Database for Small Molecules. *J. Chem. Theory Comput.* **2017**, *13*, 6237–6252.

- (191) Spezia, R.; Knecht, S.; Mennucci, B. Excited State Characterization of Carbonyl Containing Carotenoids: a Comparison Between Single and Multireference Descriptions. *Phys. Chem. Chem. Phys.* **2017**, *19*, 17156–17166.
- (192) Wiebeler, C.; Borin, V.; Sanchez de Araujo, A. V.; Schapiro, I.; Borin, A. C. Excitation Energies of Canonical Nucleobases Computed by Multiconfigurational Perturbation Theories. *Photochem. Photobiol.* **2017**, *93*, 888–902.
- (193) Shi, B.; Nachtigallová, D.; Aquino, A. J.; Machado, F. B.; Lischka, H. Excited States and Excitonic Interactions in Prototypic Polycyclic Aromatic Hydrocarbon Dimers as Models for Graphitic Interactions in Carbon Dots. *Phys. Chem. Chem. Phys.* **2019**, *21*, 9077–9088.
- (194) Stoneburner, S. J.; Shen, J.; Ajala, A. O.; Piecuch, P.; Truhlar, D. G.; Gagliardi, L. Systematic Design of Active Spaces for Multi-Reference Calculations of Singlet–Triplet Gaps of Organic Diradicals, with Benchmarks Against Doubly Electron-Attached Coupled-Cluster Data. *J. Chem. Phys.* **2017**, *147*.
- (195) Loos, P.-F.; Boggio-Pasqua, M.; Scemama, A.; Caffarel, M.; Jacquemin, D. Reference Energies for Double Excitations. *J. Chem. Theory Comput.* **2019**, *15*, 1939–1956.
- (196) Schreiber, M.; Silva-Junior, M. R.; Sauer, S. P. A.; Thiel, W. Benchmarks for Electronically Excited States: CASPT2, CC2, CCSD, and CC3. *J. Chem. Phys.* **2008**, *128*, 134110.
- (197) Scott, T.; Nieman, R.; Luxon, A.; Zhang, B.; Lischka, H.; Gagliardi, L.; Parish, C. A. A Multireference *ab initio* Study of the Diradical Isomers of Pyrazine. *J. Phys. Chem. A* **2019**, *123*, 2049–2057.
- (198) Marie, A.; Loos, P.-F. Reference Energies for Valence Ionizations and Satellite Transitions. *J. Chem. Theory Comput.* **2024**,

- (199) Grimme, S.; Neese, F. Double-Hybrid Density Functional Theory for Excited Electronic States of Molecules. *J. Chem. Phys.* **2007**, *127*, 154116.
- (200) Li, Z.; Liu, W. Critical Assessment of TD-DFT for Excited States of Open-Shell Systems: I. Doublet–Doublet Transitions. *J. Chem. Theory Comput.* **2016**, *12*, 238–260.
- (201) Li, Z.; Liu, W. Critical Assessment of Time-dependent Density Functional Theory for Excited States of Open-Shell Systems: II. Doublet-Quartet Transitions. *J. Chem. Theory Comput.* **2016**, *12*, 2517–2527.
- (202) Maurice, D.; Head-Gordon, M. Configuration Interaction with Single Substitutions for Excited States of Open-shell Molecules. *Int. J. Quantum Chem.* **1995**, *56*, 361–370.
- (203) Drabik, G.; Szklarzewicz, J.; Radoń, M. Spin-State Energetics of Metallocenes: How Do Best Wave Function and Density Functional Theory Results Compare with the Experimental Data? *Phys. Chem. Chem. Phys.* **2021**, *23*, 151–172.
- (204) Aoto, Y. A.; de Lima Batista, A. P.; Kohn, A.; de Oliveira-Filho, A. G. How to Arrive at Accurate Benchmark Values for Transition Metal Compounds: Computation or Experiment? *J. Chem. Theory Comput.* **2017**, *13*, 5291–5316.
- (205) Escudero, D.; Thiel, W. Assessing the Density Functional Theory-based Multireference Configuration Interaction (DFT/MRCI) Method for Transition Metal Complexes. *J. Chem. Phys.* **2014**, *140*.
- (206) Huntington, L. M.; Nooijen, M. Application of Multireference Equation of Motion Coupled-cluster Theory to Transition Metal Complexes and an Orbital Selection Scheme for the Efficient Calculation of Excitation Energies. *J. Chem. Phys.* **2015**, *142*.
- (207) Jacquemin, D.; Kossoski, F.; Gam, F.; Boggio-Pasqua, M.; Loos, P.-F. Reference Vertical Excitation Energies for Transition Metal Compounds. *J. Chem. Theory Comput.* **2023**, *19*, 8782–8800.

- (208) Suo, B.; Shen, K.; Li, Z.; Liu, W. Performance of TD-DFT for Excited States of Open-Shell Transition Metal Compounds. *J. Phys. Chem. A* **2017**, *121*, 3929–3942.
- (209) Radoń, M. Benchmarking Quantum Chemistry Methods for Spin-State Energetics of Iron Complexes Against Quantitative Experimental Data. *Phys. Chem. Chem. Phys.* **2019**, *21*, 4854–4870.
- (210) Khedkar, A.; Roemelt, M. Modern Multireference Methods and Their Application in Transition Metal Chemistry. *Phys. Chem. Chem. Phys.* **2021**, *23*, 17097–17112.
- (211) Li, R.; Zheng, J.; Truhlar, D. G. Density Functional Approximations for Charge Transfer Excitations with Intermediate Spatial Overlap. *Phys. Chem. Chem. Phys.* **2010**, *12*, 12697–12701.
- (212) Tuna, D.; Lu, Y.; Koslowski, A.; Thiel, W. Semiempirical Quantum-chemical Orthogonalization-Corrected Methods: Benchmarks of Electronically Excited States. *J. Chem. Theory Comput.* **2016**, *12*, 4400–4422.
- (213) Van Dijk, J.; Casanova-Páez, M.; Goerigk, L. Assessing Recent Time-Dependent Double-Hybrid Density Functionals on Doublet–Doublet Excitations. *ACS Phys. Chem. Au* **2022**, *2*, 407–416.
- (214) Kossoski, F.; Loos, P.-F. State-specific configuration interaction for excited states. *J. Chem. Theory Comput.* **2023**, *19*, 2258–2269.
- (215) Harbach, P. H.; Wormit, M.; Dreuw, A. The Third-order Algebraic Diagrammatic Construction Method (ADC(3)) for the Polarization Propagator for Closed-shell Molecules: Efficient Implementation and Benchmarking. *J. Chem. Phys.* **2014**, *141*, 064113.
- (216) Watson Jr, T. J.; Lotrich, V. F.; Szalay, P. G.; Perera, A.; Bartlett, R. J. Benchmarking

- for Perturbative Triple-Excitations in EE-EOM-CC Methods. *J. Phys. Chem. A* **2013**, *117*, 2569–2579.
- (217) Kánnár, D.; Szalay, P. G. Benchmarking Coupled Cluster Methods on Valence Singlet Excited States. *J. Chem. Theory Comput.* **2014**, *10*, 3757–3765.
- (218) Kánnár, D.; Tajti, A.; Szalay, P. G. Accuracy of Coupled Cluster Excitation Energies in Diffuse Basis Sets. *J. Chem. Theory Comput.* **2017**, *13*, 202–209.
- (219) Silva-Junior, M. R.; Schreiber, M.; Sauer, S. P.; Thiel, W. Benchmarks for Electronically Excited States: Time-dependent Density Functional Theory and Density Functional Theory Based Multireference Configuration Interaction. *J. Chem. Phys.* **2008**, *129*, 104103.
- (220) Rohrdanz, M. A.; Martins, K. M.; Herbert, J. M. A Long-range-corrected Density Functional That Performs Well for Both Ground-State Properties and Time-dependent Density Functional Theory Excitation Energies, Including Charge-transfer Excited States. *J. Chem. Phys.* **2009**, *130*, 054112.
- (221) Jacquemin, D.; Perpète, E. A.; Ciofini, I.; Adamo, C. Assessment of Functionals for TD-DFT Calculations of Singlet–Triplet Transitions. *J. Chem. Theory Comput.* **2010**, *6*, 1532–1537.
- (222) Jacquemin, D.; Perpète, E. A.; Ciofini, I.; Adamo, C.; Valero, R.; Zhao, Y.; Truhlar, D. G. On the Performances of the M06 Family of Density Functionals for Electronic Excitation Energies. *J. Chem. Theory Comput.* **2010**, *6*, 2071–2085.
- (223) Mardirossian, N.; Parkhill, J. A.; Head-Gordon, M. Benchmark Results for Empirical Post-gga Functionals: Difficult Exchange Problems and Independent Tests. *Phys. Chem. Chem. Phys.* **2011**, *13*, 19325–19337.

- (224) Jacquemin, D.; Perpète, E. A.; Ciofini, I.; Adamo, C. Assessment of the ω B97 Family for Excited-State Calculations. *Theor. Chem. Acc.* **2011**, *128*, 127–136.
- (225) Huix-Rotllant, M.; Ipatov, A.; Rubio, A.; Casida, M. E. Assessment of Dressed Time-Dependent Density-Functional Theory for the Low-lying Valence States of 28 Organic Chromophores. *Chem. Phys.* **2011**, *391*, 120–129.
- (226) Della Sala, F.; Fabiano, E. Accurate Singlet and Triplet Excitation Energies Using the Localized Hartree–Fock Kohn–Sham Potential. *Chem. Phys.* **2011**, *391*, 19–26.
- (227) Trani, F.; Scalmani, G.; Zheng, G.; Carnimeo, I.; Frisch, M. J.; Barone, V. Time-dependent Density Functional Tight Binding: New Formulation and Benchmark of Excited States. *J. Chem. Theory Comput.* **2011**, *7*, 3304–3313.
- (228) Peverati, R.; Truhlar, D. G. Performance of the M11 and M11-L Density Functionals for Calculations of Electronic Excitation Energies by Adiabatic Time-dependent Density Functional Theory. *Phys. Chem. Chem. Phys.* **2012**, *14*, 11363–11370.
- (229) Maier, T. M.; Bahmann, H.; Arbuznikov, A. V.; Kaupp, M. Validation of Local Hybrid Functionals for TDDFT Calculations of Electronic Excitation Energies. *J. Chem. Phys.* **2016**, *144*, 074106.
- (230) Sauer, S. P.; Pitzner-Frydendahl, H. F.; Buse, M.; Jensen, H. J. A.; Thiel, W. Performance of SOPPA-Based Methods in the Calculation of Vertical Excitation Energies and Oscillator Strengths. *Mol. Phys.* **2015**, *113*, 2026–2045.
- (231) Yang, Y.; Peng, D.; Lu, J.; Yang, W. Excitation Energies From Particle-particle Random Phase Approximation: Davidson Algorithm and Benchmark Studies. *J. Chem. Phys.* **2014**, *141*, 124104.
- (232) Sauer, S. P.; Schreiber, M.; Silva-Junior, M. R.; Thiel, W. Benchmarks for Electronically Excited States: a Comparison of Noniterative and Iterative Triples Corrections

- in Linear Response Coupled Cluster Methods: CCSDR(3) Versus CC3. *J. Chem. Theory Comput.* **2009**, *5*, 555–564.
- (233) Demel, O.; Datta, D.; Nooijen, M. Additional Global Internal Contraction in Variations of Multireference Equation of Motion Coupled Cluster Theory. *J. Chem. Phys.* **2013**, *138*, 134108.
- (234) Piecuch, P.; Hansen, J. A.; Ajala, A. O. Benchmarking the Completely Renormalised Equation-of-Motion Coupled-cluster Approaches for Vertical Excitation Energies. *Mol. Phys.* **2015**, *113*, 3085–3127.
- (235) Tajti, A.; Szalay, P. G. Investigation of the Impact of Different Terms in the Second Order Hamiltonian on Excitation Energies of Valence and Rydberg States. *J. Chem. Theory Comput.* **2016**, *12*, 5477–5482.
- (236) Rishi, V.; Perera, A.; Nooijen, M.; Bartlett, R. J. Excited States From Modified Coupled Cluster Methods: Are They Any Better Than EOM CCSD? *J. Chem. Phys.* **2017**, *146*, 144104.
- (237) Dutta, A. K.; Nooijen, M.; Neese, F.; Izsák, R. Exploring the Accuracy of a Low Scaling Similarity Transformed Equation of Motion Method for Vertical Excitation Energies. *J. Chem. Theory Comput.* **2018**, *14*, 72–91.
- (238) Kossoski, F.; Boggio-Pasqua, M.; Loos, P.-F.; Jacquemin, D. Reference Energies for Double Excitations: Improvement and Extension. *J. Chem. Theory Comput.* **2024**, *20*, 5655–5678.
- (239) Loos, P.-F.; Lipparini, F.; Matthews, D. A.; Blondel, A.; Jacquemin, D. A Mountaineering Strategy to Excited States: Revising Reference Values with EOM-CC4. *J. Chem. Theory Comput.* **2022**, *18*, 4418–4427.

- (240) Hoyer, C. E.; Ghosh, S.; Truhlar, D. G.; Gagliardi, L. Multiconfiguration Pair-Density Functional Theory Is as Accurate as CASPT2 for Electronic Excitation. *J. Phys. Chem. Lett.* **2016**, *7*, 586–591.
- (241) Sarkar, R.; Loos, P.-F.; Boggio-Pasqua, M.; Jacquemin, D. Assessing the Performances of CASPT2 and NEVPT2 for Vertical Excitation Energies. *J. Chem. Theory Comput.* **2022**, *18*, 2418–2436.
- (242) Schapiro, I.; Sivalingam, K.; Neese, F. Assessment of N-electron Valence State Perturbation Theory for Vertical Excitation Energies. *J. Chem. Theory Comput.* **2013**, *9*, 3567–3580.
- (243) Silva-Junior, M. R.; Schreiber, M.; Sauer, S. P.; Thiel, W. Benchmarks of Electronically Excited States: Basis Set Effects on CASPT2 Results. *J. Chem. Phys.* **2010**, *133*, 174318.
- (244) Helmich-Paris, B. Benchmarks for Electronically Excited States with CASSCF Methods. *J. Chem. Theory Comput.* **2019**, *15*, 4170–4179.
- (245) Huntington, L. M.; Demel, O.; Nooijen, M. Benchmark Applications of Variations of Multireference Equation of Motion Coupled-Cluster Theory. *J. Chem. Theory Comput.* **2016**, *12*, 114–132.
- (246) Zielinski, P.; Black, J. A.; Köhn, A. Performance Tests of the Second-Order Approximate Internally Contracted Multireference Coupled-Cluster Singles and Doubles Method icMRCC2. *J. Chem. Theory Comput.* **2023**, *19*, 8671–8688.
- (247) Battaglia, S.; Fransén, L.; Fdez. Galván, I.; Lindh, R. Regularized CASPT2: An Intruder-State-Free Approach. *J. Chem. Theory Comput.* **2022**, *18*, 4814–4825.
- (248) Battaglia, S.; Lindh, R. Extended Dynamically Weighted CASPT2: The Best of Two Worlds. *J. Chem. Theory Comput.* **2020**, *16*, 1555–1567.

- (249) Jagau, T.-C.; Gauss, J. Ground and Excited State Geometries via Mukherjee's Multireference Coupled-Cluster Method. *Chem. Phys.* **2012**, *401*, 73–87.
- (250) Drwal, D.; Beran, P.; Hapka, M.; Modrzejewski, M.; Sokół, A.; Veis, L.; Pernal, K. Efficient Adiabatic Connection Approach for Strongly Correlated Systems: Application to Singlet–Triplet Gaps of Biradicals. *J. Phys. Chem. Lett.* **2022**, *13*, 4570–4578.
- (251) Boggio-Pasqua, M.; Jacquemin, D.; Loos, P.-F. Benchmarking CASPT3 Vertical Excitation Energies. *J. Chem. Phys.* **2022**, *157*.
- (252) Kossoski, F.; Loos, P.-F. Seniority and Hierarchy Configuration Interaction for Radicals and Excited States. *J. Chem. Theory Comput.* **2023**, *19*, 8654–8670.
- (253) Grimme, S.; Izgorodina, E. I. Calculation of 0–0 Excitation Energies of Organic Molecules by CIS(D) Quantum Chemical Methods. *Chem. Phys.* **2004**, *305*, 223–230.
- (254) Loos, P.-F.; Jacquemin, D. Evaluating 0–0 Energies with Theoretical Tools: A Short Review. *ChemPhotoChem* **2019**, *3*, 684–696.
- (255) Zhang, N.; Liu, W.; Hoffmann, M. R. Iterative Configuration Interaction with Selection. *J. Chem. Theory Comput.* **2020**, *16*, 2296–2316.
- (256) Zhang, N.; Liu, W.; Hoffmann, M. R. Further Development of iCIPT2 for Strongly Correlated Electrons. *J. Chem. Theory Comput.* **2021**, *17*, 949–964.
- (257) Angeli, C.; Cimiraglia, R.; Evangelisti, S.; Leininger, T.; Malrieu, J.-P. Introduction of N-electron Valence States for Multireference Perturbation Theory. *J. Chem. Phys.* **2001**, *114*, 10252–10264.
- (258) Angeli, C.; Borini, S.; Cestari, M.; Cimiraglia, R. A quasidegenerate formulation of the second order n-electron valence state perturbation theory approach. *J. Chem. Phys.* **2004**, *121*, 4043–4049.

- (259) Liu, W.; Hoffmann, M. R. SDS: the ‘static-dynamic-static’ Framework for Strongly Correlated Electrons. *Theor. Chem. Acc* **2014**, *133*, 1481.
- (260) Lei, Y.; Liu, W.; Hoffmann, M. R. Further Development of SDSPT2 for Strongly Correlated Electrons. *Mol. Phys.* **2017**, *115*, 2696–2707.
- (261) Suo, B.; Lei, Y.; Han, H.; Wang, Y. Development of Xi’an-CI Package – Applying the Hole-Particle Symmetry in Multi-Reference Electronic Correlation Calculations. *Mol. Phys.* **2018**, *116*, 1051–1064.
- (262) Li, Z.; Liu, W. Spin-Adapted Open-Shell Random Phase Approximation and Time-Dependent Density Functional Theory. I. Theory. *J. Chem. Phys.* **2010**, *133*, 064106.
- (263) Li, Z.; Liu, W.; Zhang, Y.; Suo, B. Spin-Adapted Open-Shell Time-Dependent Density Functional Theory. II. Theory and Pilot Application. *J. Chem. Phys.* **2011**, *134*, 134101.
- (264) Li, Z.; Liu, W. Spin-adapted open-shell time-dependent density functional theory. III. An even better and simpler formulation. *J. Chem. Phys.* **2011**, *135*, 194106.
- (265) Liu, W. Perspective: Simultaneous Treatment of Relativity, Correlation, and QED. *WIREs Comput. Mol. Sci.* **2023**, *13*, e1652.
- (266) Liu, W.; Hoffmann, M. R. iCI: Iterative CI Toward Full CI. *J. Chem. Theory Comput.* **2016**, *12*, 1169–1178, (E) **2016**, *12*, 3000.
- (267) Pople, J.; Seeger, R.; Krishnan, R. Variational Configuration Interaction Methods and Comparison with Perturbation Theory. *Int. J. Quantum Chem.* **1977**, *12*, 149–163.
- (268) Liu, W.; Hong, G.; Dai, D.; Li, L.; Dolg, M. The Beijing Four-Component Density Functional Program Package (BDF) and Its Application to EuO, EuS, YbO and YbS. *Theor. Chem. Acc* **1997**, *96*, 75–83.

- (269) Liu, W.; Wang, F.; Li, L. The Beijing Density Functional (BDF) Program Package: Methodologies and Applications. *J. Theor. Comput. Chem.* **2003**, *2*, 257–272.
- (270) Liu, W.; Wang, F.; Li, L. In *Recent Advances in Relativistic Molecular Theory*; Hirao, K., Ishikawa, Y., Eds.; World Scientific: Singapore, 2004; pp 257–282.
- (271) Liu, W.; Wang, F.; Li, L. In *Encyclopedia of Computational Chemistry*; von Ragué Schleyer, P., Allinger, N. L., Clark, T., Gasteiger, J., Kollman, P. A., Schaefer III, H. F., Eds.; Wiley: Chichester, UK, 2004.
- (272) Zhang, Y.; Suo, B.; Wang, Z.; Zhang, N.; Li, Z.; Lei, Y.; Zou, W.; Gao, J.; Peng, D.; Pu, Z.; Xiao, Y.; Sun, Q.; Wang, F.; Ma, Y.; Wang, X.; Guo, Y.; Liu, W. Bdf: A Relativistic Electronic Structure Program Package. *J. Chem. Phys.* **2020**, *152*, 064113.
- (273) Dunning Jr, T. H. Gaussian Basis Sets for Use in Correlated Molecular Calculations. I. The Atoms Boron Through Neon and Hydrogen. *J. Chem. Phys.* **1989**, *90*, 1007–1023.
- (274) Kendall, R. A.; Dunning Jr, T. H.; Harrison, R. J. Electron Affinities of the First-Row Atoms Revisited. Systematic Basis Sets and Wave Functions. *J. Chem. Phys.* **1992**, *96*, 6796–6806.
- (275) Woon, D. E.; Dunning Jr, T. H. Gaussian Basis Sets for Use in Correlated Molecular Calculations. III. The Atoms Aluminum Through Argon. *The Journal of chemical physics* **1993**, *98*, 1358–1371.
- (276) Dyall, K. G. The Choice of a Zeroth-order Hamiltonian for Second-order Perturbation Theory with a Complete Active Space Self-Consistent-Field Reference Function. *J. Chem. Theory Comput.* **1995**, *102*, 4909–4918.
- (277) Becke, A. Accurate Local Approximation to the Exchange-correlation Density Func-

- tional: the MN12-L Functional for Electronic Structure Calculations in Chemistry and Physics. *Opt. Phys.* **1988**, *38*, 3098–3100.
- (278) Lee; Yang; Parr Development of the Colle-Salvetti Correlation-energy Formula Into a Functional of the Electron Density. *Phys. Rev. B: Condens. Matter* **1988**, *37*, 785–789.
- (279) Becke, A. Density-Functional Thermochemistry. III. The Role of Exact Exchange. *J. Chem. Phys.* **1993**, *98*, 5648–52.
- (280) Castiglioni, L.; Bach, A.; Chen, P. Spectroscopy and Dynamics of A [2b_1] Allyl Radical. *Phys. Chem. Chem. Phys.* **2006**, *8*, 2591–2598.
- (281) Huber, K.-P. *Molecular spectra and molecular structure*; Van Nostrand Reinhold New York, 1979; Vol. 4; pp 146–291.
- (282) Herzberg, G. *Electronic Spectra and Electronic Structure of Polyatomic Molecules*; Molecular Spectra and Molecular Structure; Van Nostrand: New York, 1966; Vol. III.
- (283) Slipchenko, L. V.; Krylov, A. I. Spin-conserving and Spin-flipping Equation-of-motion Coupled-cluster Method with Triple Excitations. *J. Chem. Phys.* **2005**, *123*.
- (284) Herzberg, G.; Mrozowski, S. *Molecular Spectra and Molecular Structure. I. Spectra of Diatomic Molecules*; D.Van Nostrand Co, 1950.
- (285) Ramsay, D.; Winnewisser, M. The Electronic Absorption Spectrum of the CNO Free Radical in the Gas Phase. *Chem. Phys. Lett.* **1983**, *96*, 502–504.
- (286) Grimminger, R.; Sheridan, P. M.; Clouthier, D. J. An Experimental and *ab initio* Study of the Electronic Spectrum of the Jet-cooled F₂BO Free Radical. *J. Chem. Phys.* **2014**, *140*, 164302.

- (287) Jin, B.; Sheridan, P. M.; Clouthier, D. J. Applied Quantum Chemistry: Spectroscopic Detection and Characterization of the F₂BS and Cl₂BS Free Radicals in the Gas Phase. *J. Chem. Phys.* **2015**, *142*, 124301.
- (288) Grimminger, R. A.; Clouthier, D. J.; Tarroni, R. Heavy Atom Nitroxyl Radicals. V. An Experimental and *ab initio* Study of the Previously Unknown H₂PS Free Radical. *J. Chem. Phys.* **2011**, *135*, 214306.
- (289) Wu, M.; Northrup, F. J.; Sears, T. J. Study of Renner–Teller, Spin–orbit, and Fermi-resonance Interactions in $\tilde{x}^2\pi (v_1v_20)$ Levels of NCO by Stimulated Emission Pumping Spectroscopy. *J. Chem. Phys.* **1992**, *97*, 4583–4595.
- (290) Hirota, E.; Kakimoto, M. Doppler-limited Dye Laser Excitation Spectroscopy of the PH₂ Radical: the $\tilde{a}^2a_1(000)$ – $\tilde{x}^2b_1(000)$ Band. *J. Mol. Struct.* **1995**, *352*, 379–387.
- (291) Shahu, M.; Yang, C.-H.; Pibel, C. D.; McIlroy, A.; Taatjes, C. A.; Halpern, J. B. Vinyl Radical Visible Spectroscopy and Excited State Dynamics. *J. Chem. Phys.* **2002**, *116*, 8343–8352.
- (292) Strinati, G. Application of the Green's Functions Method to the Study of the Optical Properties of Semiconductors. *La Riv. del Nuovo Cim.* **1988**, *11*, 1–86.
- (293) Lei, Y.; Suo, B.; Liu, W. iCAS: Imposed Automatic Selection and Localization of Complete Active Spaces. *J. Chem. Theor. Comput.* **2021**, *17*, 4846–4859.
- (294) Fischer, I.; Chen, P. Allyl-a Model System for the Chemical Dynamics of Radicals. *J. Phys. Chem. A* **2002**, *106*, 4291–4300.
- (295) Currie, C.; Ramsay, D. Electronic Absorption Spectrum and Dissociation Energy of the Allyl Radical. *J. Chem. Phys.* **1966**, *45*, 488–491.
- (296) Houle, F.; Beauchamp, J. Detection and Investigation of Allyl and Benzyl Radicals by Photoelectron Spectroscopy. *J. Am. Chem. Soc.* **1978**, *100*, 3290–3294.

- (297) Schüßler, T.; Deyerl, H.-J.; Dümmler, S.; Fischer, I.; Alcaraz, C.; Elhanine, M. The Vacuum Ultraviolet Photochemistry of the Allyl Radical Investigated Using Synchrotron Radiation. *J. Chem. Phys.* **2003**, *118*, 9077–9080.
- (298) Aquilante, F.; Jensen, K. P.; Roos, B. O. The Allyl Radical Revisited: a Theoretical Study of the Electronic Spectrum. *Chem. Phys. Lett.* **2003**, *380*, 689–698.
- (299) Mach, T. J.; King, R. A.; Crawford, T. D. A Coupled Cluster Benchmark Study of the Electronic Spectrum of the Allyl Radical. *J. Phys. Chem. A* **2010**, *114*, 8852–8857.
- (300) Matsika, S.; Yarkony, D. R. Beyond Two-state Conical Intersections. Three-state Conical Intersections in Low Symmetry Molecules: The Allyl Radical. *J. Am. Chem. Soc.* **2003**, *125*, 10672–10676.
- (301) Gasser, M.; Frey, J. A.; Hostettler, J. M.; Bach, A.; Chen, P. Vibronic Structure of the 3s and 3p Rydberg States of the Allyl Radical. *J. Phys. Chem. A* **2010**, *114*, 4704–4711.
- (302) Gasser, M.; Schulenburg, A. M.; Dietiker, P. M.; Bach, A.; Merkt, F.; Chen, P. Single-photon and Resonance-enhanced Multiphoton Threshold Ionization of the Allyl Radical. *J. Chem. Phys.* **2009**, *131*, 014304.